Vedolizumab and ART in recent HIV-1 infection unveil the role of α4β7 in reservoir size

Maria Reyes Jimenez-Leon, … , Luis F. Lopez-Cortes, Ezequiel Ruiz-Mateos

Clinical Medicine In-Press Preview AIDS/HIV Immunology

We evaluated the safety and viral rebound, after analytical treatment interruption (ATI), of vedolizumab and ART in recent HIV-1 infection. We used this model to analyze the impact of α4β7 on the HIV-1 reservoir size. Participants started ART with monthly Vedolizumab infusions and ATI was performed at week 24. Biopsies were obtained from ileum and caecum at baseline and week 24. Vedolizumab levels, HIV-1 reservoir, flow cytometry and cell-sorting and antibody competition experiments were assayed. Vedolizumab was safe and well-tolerated. No participant achieved undetectable viremia off ART 24 weeks after ATI. Only a modest effect on the time to achieve >1000 HIV-RNA copies/mL and the proportion of participants off ART was observed, being higher compared to historical controls. Just before ATI, α4β7 expression was associated with HIV-1 DNA and RNA in peripheral blood and with PD1 and TIGIT levels. Importantly, a complete blocking of α4β7 was observed on peripheral CD4$^+$ T-cells but not in gut (ileum and caecum), where α4β7 blockade and vedolizumab levels were inversely associated with HIV-1 DNA. Our findings support α4β7 as an important determinant in HIV-1 reservoir size, suggesting the complete α4β7 blockade in tissue as […]

Find the latest version:

https://jci.me/182312/pdf

1 **VEDOLIZUMAB AND ART IN RECENT HIV-1 INFECTION UNVEIL THE ROLE OF α4β7 IN**

2 **RESERVOIR SIZE**

3 Maria Reyes Jimenez-Leon[1*], Carmen Gasca-Capote[1*], Cristina Roca-Oporto[1], Nuria

4 Espinosa[1], Salvador Sobrino[2], Maria Fontillon-Alberdi[3], Ce Gao[4,5], Isabelle Roseto[4,5],

5 Gregory Gladkov[4,5], Inmaculada Rivas-Jeremias[1], Karin Neukam[1], Jose German Sanchez-

6 Hernandez[6], Raul Rigo-Bonnin[7], Antonio J. Cervera-Barajas[8], Rosario Mesones[8], Federico

7 García[9], Ana Isabel Alvarez-Rios[10], Sara Bachiller[1], Joana Vitalle[1], Alberto Perez-Gomez[1],

8 María Ines Camacho-Sojo[1], Isabel Gallego[1], Christian Brander[11], Ian McGowan[11], Beatriz

9 Mothe[12,13], Pompeyo Viciana[1], Xu Yu[4,5], Mathias Lichterfeld[4,5], Luis F. Lopez-Cortes[1],

10 Ezequiel Ruiz-Mateos[1#].

11   1. Institute of Biomedicine of Seville (IBiS), Virgen del Rocío University Hospital, CSIC, University of

12   Seville, Clinical Unit of Infectious Diseases, Microbiology and Parasitology, Seville, Spain

13   2.   Digestive Service, Virgen del Rocío University Hospital, Seville, Spain.

14   3. Service of Pathological Anatomy, Virgen del Rocío University Hospital, Seville, Spain.

15   4. Ragon Institute of MGH, MIT and Harvard, Cambridge, MA, USA.

16   5. Infectious Disease Division, Brigham and Women's Hospital, Boston, MA, USA.

17   6. Pharmacy service, University Hospital of Salamanca-IBSAL, Salamanca. Spain.

18   7. Department of Clinical Laboratory, Hospital Universitari de Bellvitge, IDIBELL, Universitat de

19   Barcelona, Barcelona, Spain.

20   8. Clinical Trials Units, Virgen del Rocío University Hospital, Sevilla, Spain.

21   9. Departament of Microbiology, San Cecilio University Hospital, Instituto de Investigación Ibs,

22   Granada, Ciber de Enfermedades Infecciosas, CIBERINFEC, Granada, Spain.

23   10. Biochemistry Service, Virgen del Rocío University Hospital, Seville, Spain.

24   11. AELIX Therapeutics S.L, Barcelona, Spain.

25   12. Infectious Diseases Department & IrsiCaixa AIDS Research Institute, Hospital Germans Trias I

26   Pujol, Badalona, Spain

27   13. CIBERINFEC, Spain

28

29 [*]These authors contributed equally to this work. We decided to list the PhD first and the

30 PhD student second.

31

32 [#]**Corresponding Author:** Ezequiel Ruiz-Mateos Carmona eruizmateos-ibis@us.es.

33 Laboratory of Immunovirology (Lab 211), Institute of Biomedicine of Seville (IBIS). Virgen

34 del Rocío University Hospital. Avda. Manuel Siurot s/n. PC 41013, Seville, Spain.

35

36   **Running head:** Role of α4β7 in HIV-1 reservoir size

37

38   **Conflict of interest statement:** "The authors have declared that no conflict of interest

39   exists".

40   Part of the results of this manuscript were accepted at 29th Conference on Retroviruses

41   and Opportunistic Infections (CROI) 2022.

42

43

44

ABSTRACT

We evaluated the safety and viral rebound, after analytical treatment interruption (ATI), of vedolizumab and ART in recent HIV-1 infection. We used this model to analyze the impact of α4β7 on the HIV-1 reservoir size. Participants started ART with monthly Vedolizumab infusions and ATI was performed at week 24. Biopsies were obtained from ileum and caecum at baseline and week 24. Vedolizumab levels, HIV-1 reservoir, flow cytometry and cell-sorting and antibody competition experiments were assayed. Vedolizumab was safe and well-tolerated. No participant achieved undetectable viremia off ART 24 weeks after ATI. Only a modest effect on the time to achieve >1000 HIV-RNA copies/mL and the proportion of participants off ART was observed, being higher compared to historical controls. Just before ATI, α4β7 expression was associated with HIV-1 DNA and RNA in peripheral blood and with PD1 and TIGIT levels. Importantly, a complete blocking of α4β7 was observed on peripheral CD4+ T-cells but not in gut (ileum and caecum), where α4β7 blockade and vedolizumab levels were inversely associated with HIV-1 DNA. Our findings support α4β7 as an important determinant in HIV-1 reservoir size, suggesting the complete α4β7 blockade in tissue as a promising tool for HIV-cure combination strategies.

KEYWORDS

Vedolizumab; HIV-1; reservoir; α4β7

INTRODUCTION

Antiretroviral therapy (ART) suppresses HIV-1 replication to undetectable plasma levels but fails to eradicate the virus (1). HIV-1 remains transcriptionally active, primarily from defective HIV proviruses(2), or latent in anatomical and cellular reservoirs (3, 4). However, HIV rebounds after ART interruption in most people living with HIV (PLWH) (5, 6). Therapeutic strategies are being explored to achieve the HIV eradication or permanent viral remission in the absence of ART, as occurs in persistent HIV-1 controllers (7). HIV-1 preferentially infects activated memory CD4+ T-cells, which are enriched in gastrointestinal tissues (GITs) (8, 9). One of the pathways used by CD4+ T-cells for trafficking into GITs is the interaction between α4β7 integrin, expressed on CD4+ T-cells, with the mucosal vascular addressin cell adhesion molecule 1 (MAdCAM-1), expressed primarily on high endothelial venules within GITs (10). Additionally, α4β7 integrin is also incorporated in HIV-1 virions (11). HIV-1 gp120 can bind to α4β7 integrin, expressed on CD4+ T-cells, leading to a rapid activation of lymphocyte function-associated antigen 1 (LFA-1), the integrin involved in the establishment of virological "synapses" and promoting cell-to-cell transmission of infection (12). These are key aspects in HIV-1 immunopathogenesis that need to be tackled to achieve a sustained virological remission since a high number of the target cells for HIV-1-infection are in the GITs. In this sense, CD4+α4β7+ T-cells were found to harbor three times more simian immunodeficiency viruses (SIV) DNA than α4β7- T-cells subsets (13). Besides, it has been shown that high levels of CD4+α4β7+ T-cells increased the susceptibility to HIV-1 infection in nonhuman primates and heterosexual women (14–16). In addition, treatment with α4β7 blocking molecules significantly reduced SIV-DNA levels in the gut (13, 17–19). However, the impact of blocking α4β7 expression on the HIV-1 reservoir landscape in peripheral blood and tissue in humans remains uncertain. These findings led to the hypothesis that α4β7 could be targeted to achieve a permanent virological remission off ART in humans. Vedolizumab is a humanized monoclonal antibody against α4β7 that is licensed for the treatment of inflammatory bowel disease (20–22). The therapeutic role of an α4β7 monoclonal antibody in HIV cure research remains unclear. In a recent clinical trial, no sustained viral remission was found after ART and vedolizumab treatment in ART-suppressed participants with chronic HIV-infection (23)

4

98 and the seminal efficacy data generated in a non-human primate model (19) could not

99 be reproduced (24–26). In the present study, we evaluated the safety and efficacy in viral

100 rebound, after analytical treatment interruption (ATI), of vedolizumab combined with

101 ART on recently infected PLWH. None of the participants achieved undetectable viremia

102 off ART at the end of the follow-up. However, importantly, α4β7 expression was

103 associated with DNA and RNA HIV-1 levels in peripheral blood and in two gut locations

104 (ileum and caecum). In addition, α4β7 levels were associated with PD1 and TIGIT protein

105 levels, immune checkpoints molecules previously associated with the HIV-1 reservoir

106 (27). Finally, just before ATI, despite the complete α4β7 blockade on peripheral CD4+ T-

107 cells, α4β7 was not entirely blocked in the gut where the percentage of α4β7 blockade

108 and vedolizumab levels were inversely associated with HIV-1 DNA levels. Therefore,

109 using this model we describe key insights into the role of α4β7 *in vivo* in human HIV-1

110 reservoir.

111 **RESULTS**

112

113 **Participants' characteristics and safety of vedolizumab and ART in PLWH**

114 Ten PLWH naïve for ART (nine cisgender males and one cisgender female) were enrolled

115 between September 2018 and June 2019 (Fig. 1); all participants completed the study

116 follow-up period. A total of seven monthly vedolizumab infusions were administrated,

117 in addition to ART, to each participant for 24 weeks. No adverse effects were observed

118 during the infusions or post-infusion periods (Supplementary Table 1). Furthermore, no

119 participant had detectable anti-vedolizumab antibodies at baseline (BL) or throughout

120 follow-up (data not shown). Date of HIV-1 infection was estimated as the average

121 between a HIV-1 negative and HIV-1 positive serologic test (maximum time frame of six

122 months) and/or 15 days before onset of symptoms compatible with acute retroviral

123 syndrome. The median time from HIV-1 infection to study initiation was 75 (IQR: [40 to

124 82]) days. Demographic, immunological, and virological characteristics of the study

125 participants (vedolizumab group) are summarized in Table 1. In summary, vedolizumab

126 was safe and well tolerated in people that star ART and vedolizumab in recent HIV-

127 infection.

128

129 **Efficacy after the analytical treatment interruption**

130 ART and vedolizumab were interrupted at week 24 and participants were followed every

131 four weeks during the ATI period up to 24 weeks. The plasma viral load (pVL) kinetics

132 before ATI is shown in Supplementary Fig. 1a. ART was restarted when pVL was >100,000

133 HIV-1 RNA copies/mL in two consecutive measurements one month apart. All

134 participants had detectable viremia during the ATI and none achieved undetectable

135 viremia (<20 HIV-RNA copies/mL) after 24 weeks of follow-up in the absence of

136 treatment (Fig. 2a). Four participants resumed ART due to the virological criteria and the

137 other six participants completed the follow-up with pVL of 1,590 (participant 1, P1);

138 6,250 (P4); 4,670 (P6); 10,000 (P8); 36,450 (P9) and 4,300 (P10) HIV-1 RNA copies/mL at

139 week 48, respectively (Fig. 2a). Participant number seven restarted treatment at week

140 36 (12 weeks after ATI) and showed new viral recrudesce at week 40, compatible with

141 self-reported intermittent low adherence to the treatment during the whole clinical

142 trial. For that reason, participant 7 was removed from HIV-1 reservoir analysis. No ART

6

143 resistance mutations were detected at BL, week 24 and 48 in this participant (data not

144 shown). Overall, there were no decreases in CD4 T-cells counts at week 24, 28 and 48

145 compared to the BL; in fact, we observed a significant increase in CD4 T-cells counts at

146 week 24 and 28 (Supplementary Fig. 1b). We neither observed a significant decrease

147 from ATI to week 48 (Supplementary Fig. 1b). Therefore, in this study we did not see

148 sustained viral remission during ATI after 24 weeks of ART treatment and vedolizumab

149 in recently infected PLWH.

150 Subsequently, in a post hoc analysis, we compared the pVL kinetics during the ATI from

151 the vedolizumab group with historical controls from the placebo arm of the AELIX-002

152 study (NCT03204617) which also included a 24-weeks ATI (28). Both groups were

153 matched by estimated time since HIV-1 acquisition at the moment of starting ART, sex

154 and age (Table 1). At the moment of ATI, CD4+ T-cell counts and CD4/CD8 ratio were

155 higher in the historical controls, as these participants had been ART suppressed for one

156 year more than the vedolizumab group (Table 1). For the purpose of this post hoc

157 comparison, time off ART was analyzed with the same virological ART resumption

158 criteria as the vedolizumab group. We did not observe significant differences in the

159 proportion of participants remaining off ART between the two studies (Fig. 2b).

160 However, longer time to first VL>1,000 HIV-RNA copies/mL was observed in the

161 vedolizumab group (p=0.034) (Fig. 2c). Time off ART was 24 [8 – 24] and 8 [5 – 20] weeks

162 in our study and the historical control cohort, respectively (p= 0.06; Supplementary

163 Table 2). A non-significant increase in the time to reach >2000 HIV-RNA copies/mL

164 (p=0.074)was observed in the vedolizumab group, and no differences were observed in

165 the time to first VL >10000 or 20000 HIV-RNA copies/mL (p=0.333 and p=0.303,

166 respectively) (Supplementary Fig. 1c-e) and other parameters (Supplementary Table 2).

167 HLA protective alleles has been associated with the spontaneous control of HIV viremia

168 (29, 30). Individual with these alleles may bias viral rebound kinetics after ATI.

169 Considering only participants without protective HLA alleles (participants 36, 16 and 17

170 from historical control cohort and participant 4 from our study were excluded), with the

171 aim of avoiding confusing factors that could favor the viremia control, the differences

172 between pVL kinetics increased between groups. There was a a higher but not

173 significant (p=0.051) proportion of participants remaining off ART in the vedolizumab

174 group (Fig. 2d). Interestingly, the time off ART (24 [8 - 24] vs 7 [4 - 10]) and to peak VL (8

7

175 [4 - 14] vs 4 [4 - 7]) were higher in the vedolizumab group compared to the historical

176 controls (p=0.027 and p=0.047), respectively, the same as the time to first VL>1000 HIV-

177 RNA copies/mL (p=0.044) (Fig. 2e). A non-significant increase was observedin the time

178 to reach >2000 HIV-RNA copies/mL (p=0.094) in the vedolizumab group, and no

179 differences were observed in the time to first VL>10000 or 20000 HIV-RNA copies/mL

180 (p=0.263 and p=0.285, respectively). It is important to note, that VL pre-ART, in these

181 participants without protective HLA alleles, was higher in the vedolizumab group

182 compared to the historical control group (6.09 [5.12–6.90] vs 4.95 [4.43–5.73], p=0.030).

183

184 **Combined therapy resulted in decreased HIV-1 reservoir levels**

185 Next, although no sustained viral remission was found, we took advantage of the study

186 design to explore the relationship between immunological factors in the intervention

187 cohort, focusing on α4β7+ expression, and HIV-1 reservoir levels in peripheral blood and

188 GIT. Regarding HIV reservoir levels, a decrease in total HIV-1 DNA was observed in

189 PBMCs at weeks 24 and 28. (Fig. 3a, left panel). A similar pattern was observed in cell

190 associated HIV-1 RNA except for week 28 (Fig. 3a, right panel). This may be due to the

191 fact that all participants at week 28 were without ART but with detectable viral load (Fig.

192 2a). Interestingly, in all of the studied time points, participants who restarted ART (red

193 bars) showed higher levels of total HIV-1 DNA in PBMCs, than participants who reached

194 study week 48 of follow-up without ART (blue bars) (Supplementary Fig. 2a, left panel).

195 The same kinetic was observed for cell associated HIV-1 RNA but only for BL and week

196 28 (Supplementary Fig. 2a, right panel). HIV-1 reservoir was also assayed in ileum and

197 caecum cells (Fig. 3b). A significant decrease was observed in both locations in total HIV-

198 1 DNA and cell-associated HIV-1 RNA at week 24 respect to BL (Fig. 3b, left and right

199 panel, respectively). We did not observe differences in HIV-1 reservoir levels (DNA or

200 RNA) between ileum and caecum neither at BL nor week 24. Participants who restarted

201 ART (red bars) presented similar levels of HIV-1 reservoir in GIT (DNA or RNA) than those

202 who did not restart ART (blue bars) with no significant differences at BL and week 24

203 neither in ileum nor caecum (Supplementary Fig. 2b, left and right panel, respectively).

204 There was a strong positive correlation between total HIV-1 DNA reservoir in ileum and

205 caecum and the plasma viral load at BL (Fig. 3c, left panels). Interestingly, this correlation

206 was not observed with the HIV-1 reservoir (DNA or RNA) in peripheral blood (Fig. 3c,
207 right panels).

208

209 **Effect of combined therapy on β7 integrin expression**

210 The percentage of memory CD4+ T-cells expressing β7 integrin was determined
211 throughout the follow-up period. Quantification of α4β7+ levels was performed by
212 gating CD4+CD45RO+β7+ as previously described (9, 14, 31, 32). We did not observe
213 differences in neither in the percentage (Fig. 4a) nor in the absolute numbers
214 (Supplementary Fig. 3a) CD4+CD45RO+β7+ cells in PBMCs during follow-up.
215 Nevertheless, PLWH who restarted ART (red bars) had higher levels of
216 CD4+CD45RO+β7+ in PBMCs at week 24 compared to those participants who completed
217 the ATI period (blue bars) (Supplementary Fig. 4a). The same trend was observed for
218 absolute CD4+CD45RO+β7+ cell counts but at not significant level (Supplementary Fig.
219 5a). Interestingly, those participants who resume ART after ATI increased
220 CD4+CD45RO+β7+ in PBMCs at week 24/28 and these increases were associated with
221 non-significant higher viral load levels (p=0.077), total cell associated HIV-DNA (p=0.034)
222 and HIV-RNA levels (p=0.034) in PBMCs (Supplementary Fig. 4b) and higher HIV-RNA in
223 ileum (p=0.034) and HIV-DNA in caecum at BL (p=0.077) (Supplementary Fig. 4c).
224 Likewise at week 24, those participants who increased CD4+CD45RO+β7+ levels in
225 PBMCs at week 24/28, had higher CD4+CD45RO+β7+, total and defective HIV-DNA and
226 HIV-RNA levels in PBMCs at just before ATI (week 24) (Fig. 4b and Supplementary Fig.
227 4d). The same results were observed when analyzing absolute CD4+CD45RO+β7+ T-cells
228 counts (Supplementary Fig. 3b and 5b-d). In addition, cell associated HIV-RNA, total and
229 defective, but not intact HIV-1 DNA levels were also directly associated with
230 CD4+CD45RO+β7+ in PBMCs at week 24 (Fig. 4c). Furthermore, PLWH who restarted
231 ART (red bars) presented higher levels of defective HIV-1 DNA levels (Supplementary Fig.
232 4e). Unlike PBMCs (Fig. 4a), the CD4+CD45RO+β7+ subset was significant decreased in
233 ileum and caecum at week 24 respect to BL (Fig. 4d). There were no decreases in total
234 CD4+ T-cell levels in GI tissue (Supplementary Fig. 4f) and no differences were detected
235 between PLWH who restarted ART (red bars) or not (blue bars) in GI tissue at BL and
236 week 24 (Supplementary Fig. 4g).

237   To deeply analyze the importance of α4β7 integrin in the HIV reservoir levels, we also

238   determined the HIV-1 reservoir in peripheral CD4+CD45RO+β7+ and β7- sorted cells (Fig.

239   4e). CD4+CD45RO+β7+ cells presented higher levels of total HIV-1 DNA and cell

240   associated HIV-1 RNA at BL and week 24 than CD4+CD45RA+β7- cells. Although

241   statistical differences were not observed at week 24 in HIV-1 RNA levels, 33.3% were

242   positive for HIV-1 RNA levels in CD4+CD45RA+β7- cells compared to 66.6% in

243   CD4+CD45RA+β7+ cells (Fig. 4e). Interestingly, we only observed a decrease in HIV-1

244   DNA and RNA in CD4+CD45RO+β7+ cells at week 24 relative to BL (Fig. 4e).

245

246   **Inefficient α4β7-blocking in GIT is associated with higher HIV-1 reservoir levels**

247   Serum concentrations of vedolizumab were determined prior each monthly infusion and

248   at weeks 28 and 32 after ATI (Fig. 5a). The concentrations were similar to those reported

249   in clinical trials of inflammatory bowel disease (20, 21) but the median concentration was

250   slightly lower compared to the clinical trial performed in chronic HIV-1-infection(23).

251   This may occur because vedolizumab can also be bound to the α4β7 integrin present on

252   free virus envelope from participants with high detectable viremia. Using the anti-α4β7

253   mAb clone ACT-1, with the same target epitope of vedolizumab, we observed that α4β7

254   integrin was completely blocked by vedolizumab on peripheral CD4+ T-cells at week 24

255   (Fig. 5b, left panel) while partial blocking was found in ileum and caecum in the same

256   time point (Fig. 5b, right panel). Indeed, there was a positive correlation between the

257   fraction of CD4+CD45RO+α4β7+ not blocked by vedolizumab and HIV-1 DNA in ileum

258   and caecum (Fig. 5c, left panels). However, when we used the clone FIB504, which

259   epitope is recognized independently of bounded vedolizumab, we did not observe this

260   correlation (Fig. 5c, right panels). Taking this into account, we calculated the percentage

261   of blocked α4β7 with the combination of ACT-1 and FIB504 clones. There were no

262   differences in the percentage of CD4+CD45RO+α4β7+ cells blocked between ileum and

263   caecum at week 24 neither between PLWH who restarted ART (red bars) or not (blue

264   bars) (Supplementary Fig. 6a). Interestingly, we found an association between HIV-1

265   DNA reservoir and CD4+CD45RO+α4β7+ cells blocked in both ileum and caecum at the

266   same time point (Fig. 5d). Importantly, we also observed a negative correlation between

267   the HIV-1-RNA levels in ileum and vedolizumab concentration at week 20 (Fig. 5e), this

268   correlation was also observed for HIV-DNA levels on PBMCs (Supplementary Fig. 6b).

269

Immune checkpoint molecules are associated with α4β7 integrin and HIV-1 reservoir levels

Immune checkpoint molecules have been associated with HIV-1 reservoir levels(27). We quantified the expression of PD1, TIGIT, TIM3 and LAG3 in memory CD4 T-cells in PBMCs and GI tissue cells and analyzed its association with α4β7 integrin and HIV-1 reservoir levels. Following the same trend as overall α4β7 expression in peripheral blood (Fig. 4a), we did not observe differences neither in PD1 and TIGIT expression (Fig. 6a) nor LAG3 and TIM3 (Supplementary Fig. 7a) during follow-up. We observed that PD1 memory CD4+ T cell levels positively correlated with peripheral total HIV-DNA and a similar but non-significant (p=0.125) correlation was observed for TIGIT memory CD4+ T cell levels (Fig. 6b). In the same way, PD1 and TIGIT memory CD4+ T cell levels positively correlated with CD4+CD45RO+β7+ levels (Fig. 6c). We calculated the "multiple immune checkpoint phenotype" in combination with β7 integrin (simultaneous expressions of three or more of the analyzed markers). The simultaneous expression index of these markers (β7+LAG3+PD1+TIM3+TIGIT+) positively correlated with CD4+CD45RO+β7+ and peripheral total HIV-DNA (Fig. 6d), showing the highest levels in PLWH who restarted ART after ATI (Fig. 6d and Supplementary Fig. 7b). Furthermore, we analyzed whether these multiple immune checkpoints, α4β7+ expression and HIV-1 reservoir were associated with inflammation. Inflammatory soluble markers such as hsCRP, the coagulation biomarker D-Dimer (DD) and beta-2 microglobulin (B2M) were assayed (Fig. 6e). B2M levels decreased along the follow-up (Fig. 6e, right panel) and at week 24 were associated with α4β7 and PD1 memory CD4+ T-cell expression, and with HIV-1 DNA levels, which in turn were also associated with DD levels (Fig. 6f).

Finally, we also analyzed these molecules in GIT. In this case, the HLA-DR, LAG3, TIM3 (Supplementary Fig. 7c) and PD1 expression (Fig. 6g), were significantly decreased in memory CD4 T-cells at week 24 respect to BL in ileum and caecum, contrary to what occurred in peripheral blood (Fig. 6a). Follicular CD4 T-cells (Tfh) express PD1 and are enriched in α4β7 integrin (33). Although Tfh levels did not change during follow-up (Fig. 6h), at week 24, Tfh levels were positively associated with the fraction of CD4+ α4β7+

299 not blocked by vedolizumab and a non-significant positive correlation was found with

300 total HIV-1 DNA in GIT (Fig. 6i).

301

302 **Retinoic acid is associated with reservoir levels in GIT**

303 The main GITs cell subsets associated with higher α4β7 integrin expression are Tfh,

304 regulatory CD4+ T-Cells (Treg) and IL-17- producing T helper (Th17). However, we did

305 not observe associations between Treg and Th17 cell levels and α4β7 expression, in

306 contrast to Tfh cells (Fig. 6i). Dendritic cells are the major producers of retinoic acid,

307 which is required for inducing gut-tropic lymphocytes. Retinoic acid potentiates the

308 induction of gut homing FoxP3+ Tregs and inhibits the development of Th17 cells.

309 Th17/Treg cells ratio and retinoic acid are involved in the maintenance of GITs

310 homeostasis and damage (34). We found that Treg levels were significant increased and

311 consequently the ratio Th17/Treg decreased at week 24 at ileum (Fig. 7a). Although we

312 did not observe differences in retinoic acid plasma levels during follow-up

313 (Supplementary Fig. 8a), a negative correlation between total HIV-1 DNA levels in

314 caecum and retinoic acid and a positive association between Treg and myeloid dendritic

315 cells (mDCs) in caecum with retinoic acid levels were observed at week 24 (Fig. 7b).

316 Finally, changes between peripheral HIV-1 DNA reservoir levels between BL and week

317 24 (Supplementary Fig. 8b) and the Th17/Treg ratio at ileum and caecum showed a

318 positivenon-significant and significant association, respectively(Fig. 7c).

DISCUSSION

In this clinical trial, we analyzed the safety and efficacy of vedolizumab combined with ART to achieve virological remission in treatment naïve early-infected PLWH after ATI. Our results show that vedolizumab was safe and well tolerated. Nevertheless, no sustained undetectable viremia was seen during the ATI period. However, using this model we unveiled important insights about the role of α4β7 expression in HIV-1 reservoir levels in peripheral blood and gastrointestinal tissue in humans.

A previous study performed in individuals with chronic HIV-1 infection(23),using a similar regimen of vedolizumab than the one used in our study, also showed to be well tolerated, confirming a safe spectrum profile in PLWH. In the same study, vedolizumab was also not able to induce virological remission after ART interruption(23), in accordance with previous findings in the SIV model (24–26). However, the criteria for ART reintroduction after ATI in our study allowed us to observe that 60% of participants completed the ATI with no decreased CD4+ T-cell levels, and viral loads at the end of the ATI period ranging from 1,590 to 36,950 HIV-1 RNA copies/ml (median [IQR]; 5495 [3311 – 13804]). Interestingly, the proportion of participants off ART and the time to achieve > 1,000 HIV-RNA copies/mL was higher compared to an historical control group (28), especially when participants with protective alleles were removed from the analysis, as a potential confounding factor. It is important to note, that these differences were observed despite the less favorable profile of the vedolizumab group in terms of the lower time on suppressive ART and the trend to have higher pre-ART viral loads, both factors associated to a faster viral recrudescence and higher levels of viremia after ATI (35, 36). Despite this modest efficacy effect, these data support the further testing of vedolizumab in combination with other immunotherapies for HIV-cure strategies.

Our unique clinical trial design allowed us to analyze the role of α4β7 expression on peripheral blood and tissue and its impacts on HIV-1 reservoir levels after ART initiation in humans. First, we analyzed HIV-1 reservoir dynamics, cell associated HIV-DNA and RNA, on PBMCs and GITs along the follow-up. As expected, there was a fast decrease of HIV-1 reservoir in peripheral blood during the first 24 weeks after ART initiation, as it has been previously described after early ART and in contrast to what has been observed in chronically ART-suppressed individuals (37–39). In our clinical trial, study participants

350 who resumed ART early during the ATI (n=4) showed higher levels of HIV-1 reservoir,

351 total cell associated HIV-DNA and RNA, at study entry and at ATI start in contrast to

352 participants who remained off ART up to week 48 (n=6) in which peripheral HIV-1 DNA

353 levels remained lower along the study. Similarly, low viral reservoir, total cell associated

354 HIV-DNA and RNA, has been previously reported to be associated with a longer time to

355 viral rebound (35, 36). Little is known about HIV-1 reservoir dynamics in gut-associated

356 lymphoid tissue (GALT) after early ART initiation (40), due to the difficulty of obtaining

357 gut biopsies in PLWH during acute HIV-1 infection (41). In our study, we also observed a

358 sharp decrease of the HIV-1 DNA levels in GITs as it occurred in PBMCs; however, the

359 strong direct association between pre-ART plasma viral load and HIV-1 DNA levels in

360 GITs, but not with HIV-1 DNA in peripheral blood, highlights the important contribution

361 of tissue reservoir to viremia, as suggested in animal models (42).

362 The association of α4β7 levels and blocking with the modulation of HIV-1 reservoir

363 landscape in peripheral blood and tissue in humans remains unclear. Our results

364 revealed strong associations between memory CD4+α4β7+ and HIV-1 reservoir levels

365 (both, cell associated HIV-DNA and HIV-RNA) in PBMCs and in two GITs locations, ileum

366 and caecum. These results are similar to those found in a cohort of PLWH who started

367 ART during primary infection, where total HIV-1 DNA was directly associated with α4β7

368 expression in intestinal lamina propria mononuclear cells of ileum and rectum (43).

369 Additionally, we were able to distinguish that this association of α4β7 levels with

370 peripheral reservoir was mainly due to defective provirus, and not because of the intact

371 proviral reservoir(44). However, the clinical relevance of defective HIV-DNA levels came

372 from the fact that these levels were associated with further ART re-introduction after

373 ATI. Further insights into the role of α4β7 expression on HIV-1 reservoir establishment

374 came from the different α4β7 expression kinetics in peripheral blood and tissue. It is

375 known that memory CD4+ α4β7+ cells are early target of HIV-1 infection following

376 mucosal transmission (13, 14, 45, 46). We found that overall α4β7 expression on

377 peripheral CD4+ T-cells did not change during combined treatment with ART for 24

378 weeks. However, a detailed analysis of the dynamics of α4β7 expression on peripheral

379 CD4+ T-cells demonstrated that those participants who decreased CD4+ α4β7+ cells

380 before ATI achieved the lowest levels and this was associated with no recrudescent of

381 viral rebound after ATI and at the same time with lower total and defective HIV-DNA

382 and HIV-RNA levels. These results are important because based on α4β7 dynamics and

383 levels before ATI, we may predict those individuals who are going to resume ART.

384 Regarding GI tissue, a uniform down-regulation of α4β7 expression was observed on

385 ileum and caecum CD4+ T-cells during follow-up. To investigate the α4β7 block, we used

386 two different antibodies sharing or not the same epitopes of vedolizumab binding site.

387 This strategy led us to uncover that anti-α4β7 treatment completely blocks α4β7 in the

388 periphery but not in GI tissue. Interestingly, we found that the cell associated HIV-DNA

389 was strongly associated with the percentage of α4β7 not blocked on GITs memory CD4+

390 T-cells but not with total α4β7 expression. These data were supported by the higher HIV-

391 1 reservoir levels, cell associated HIV-DNA and HIV-RNA, in sorted α4β7+ peripheral

392 blood CD4+ T-cells compared to α4β7- cells in accordance with previous findings in the

393 simian model (13) and in humans in cells positive for α4β1 heterodimer that were

394 enriched in HIV-1 content compared to α4β1- cells (47). These results also open the

395 question of whether vedolizumab administration at higher doses would have increased

396 virological efficacy. In this sense, it is important to note the favorable safety profile of

397 vedolizumab compared to other immunomodulators for the development of adverse

398 events, such us progressive multifocal leukoencephalopathy (48, 49). In our study,

399 participants received monthly doses of 300 mg vedolizumab (4.3 mg/kg [3.6-5.02])

400 together with ART, the approved dose used for the treatment of IBD (20, 21). In previous

401 studies, the primatized analogue of anti-α4β7 was administered at a dose of 50 mg/kg,

402 10-fold higher than the dose of the present study, fully masking the expression of α4β7

403 expressed on the surface of lymphocytes harvested from GITs biopsies (17, 18, 50, 51).

404 These results suggest that the reduction of HIV-1 reservoir may be associated with

405 vedolizumab concentration. Indeed, we found an inverse correlation between total cell

406 associated HIV-DNA and HIV-RNA in peripheral blood and ileum, respectively, with

407 vedolizumab levels just before ATI.

408 Afterwards, we performed additional phenotypical characterization of α4β7+ CD4+ T-

409 cells and analyzed their association with HIV-1 reservoir levels. The expression of the

410 immune checkpoint molecules PD1, LAG3 and TIM3 on T-cells was also previously

411 identified as a preferential niche for the HIV-1 reservoir enrichment(27). In accordance

412 with previous studies (52), we found that the co-expressing phenotypes of these

413 immune checkpoint molecules and α4β7 expression on memory CD4+ T-cells exhibited

15

strong correlations with total cell associated HIV-DNA. These immune checkpoint molecules were identified as a strong predictor of time to viral rebound in some ATI cohorts (53). In our clinical trial, study participants who restarted ART exhibited higher levels of memory CD4+ α4β7+LAG3+PD1+TIGIT+TIM3+ T-cells at ATI time point. Interestingly, we found that this immune checkpoint molecules and α4β7+ phenotype were associated with inflammatory biomarkers, such as β2M and D-dimer levels, previously related with cell associated HIV-1 RNA (54). Besides, we found a direct association between total cell associated HIV-DNA and D-dimer and β2M levels in plasma. These results suggest a connection between HIV-1 reservoir and inflammatory parameters, potentially related with the T-cell turnover induced by the virus and the β2M shedding even in PLWH on treatment. Remarkably, we found decreased levels of LAG3, TIM3 and PD1 CD4+ T-cell in tissue during the follow-up, reflecting the decrease HIV-1 reservoir in tissue.

Finally, we analyzed immune reconstitution in GITs of the three main functional subsets of CD4+ T cells that express α4β7: Treg, Tfh and Th17 (55, 56) in relation to GITs homeostasis and HIV-1 reservoir. No reconstitution was observed in Th17 and Tfh cells. Indeed, Tfh cells, that constitutively express PD1, were associated with free, not blocked by vedolizumab, α4β7 levels with a trend towards increased HIV-1 reservoir in ileum, suggesting the preferential infection of this T-cell subset (57). Conversely, we did find enlarged Treg levels in ileum during the follow-up and, subsequently Th17/Treg ratio decreased, which has been associated with GIT homeostasis and disease progression (58, 59). Additionally, we observed that Th17/Treg ratio was associated with HIV-1 DNA reservoir changes in the periphery along the follow-up. Besides, retinoic acid, produced by dendritic cells, plays an essential role in gut homeostasis and induces the expression of α4β7 (60, 61). Furthermore, dendritic cells from GITs enhance Treg cells' differentiation in a retinoic acid-dependent manner (62) as well as convert vitamin A in retinoic acid (63). In agreement with this, our results show a direct association between retinoic acid plasma levels and myeloid dendritic and Treg cell levels in caecum tissue. This differential immune reconstitution, depending on GIT location, was concomitant with an inverse correlation at week 24 of retinoic acid plasma levels with total proviral HIV-1 DNA reservoir in the caecum. This may support the potential role of retinoic acid as a latency reversing agent (64).

446 Overall, our results are in agreement with those of the simian model, where blocking

447 α4β7 with vedolizumab together with the use of a broadly neutralizing antibody delayed

448 viral rebound after ATI (51), but also in humans, where the use of anti-α4β7 therapy was

449 associated with the attrition of lymphoid aggregates that may potentially impact HIV-1

450 reservoir levels in GIT (65).

451 One of the major limitations of this study was the low number of participants and that

452 most of the were men. However, the stringent inclusion criteria, only participants with

453 confirmed acute/recent HIV-1 infection were included, and the extensive tissue

454 sampling requirements justified the trial sample size and sex bias. Another limitation

455 was the lack of a randomized control group. However, we were able to compare the ATI

456 outcomes from our study with the placebo recipients from a recently reported study

457 performed in a very comparable population.

458 In conclusion, vedolizumab, administered for 24 weeks, was safe and well tolerated in

459 early-treated PLWH. No sustained virological remission after ART interruption was found

460 in participants treated with vedolizumab. Importantly, this clinical trial suggests that

461 α4β7 is an important determinant of HIV-1 reservoir levels seeding in peripheral blood

462 and specially in tissues in humans and therefore, supports further testing of

463 vedolizumab in combination with other compounds, as a promising tool for HIV-1 cure

464 strategies.

465

466

MATERIALS AND METHODS

Sex as a biological variable

Cisgender woman and men were included in the study

Study design

This was an open-label, single-arm phase 2 clinical trial to assess the safety and virological effect of vedolizumab (Entyvio™) and ART in participants with early HIV-1 infection and naïve for ART that underwent analytical treatment interruption (ATI) (Fig. 1). Commercially available vedolizumab and ART were supplied by Virgen del Rocío University Hospital (Seville, Spain). ART regimen was dolutegravir (DTG, 50mg), tenofovir alafenamide (TAF, 25mg) and emtricitabine (FTC, 200mg), all qd. The clinical trial was performed at the Clinic Unit of Infectious Diseases, Microbiology and Parasitology and at the Phase I/II Clinical Trials Units at Virgen del Rocío University Hospital (Seville, Spain). PLWH were eligible if they were 18 to 65 years of age. Participants were required to have a CD4+ T-cells count of > 350 cells/μl and a viremia >10^4 HIV-1 RNA copies/ml. Study participants were recruited between September 2018 and June 2019 and started ART together with 300mg of vedolizumab intravenous infusions at 0, 4, 8, 12, 16, 20 and 24 weeks. At week 24 of follow-up ART and vedolizumab treatment were interrupted. Biopsies from ileum and caecum were obtained at BL and week 24, pre-ART and pre-ATI, respectively. Throughout the treatment interruption phase, participants were monthly monitored by measuring CD4+ T-cells counts and plasma viremia. Criteria to restart ART during the ATI were a decrease in the levels of CD4 T-cells below 350 cell/μl or viral load levels above 10^5 HIV-1 RNA copies/ml (two consecutive measurements one month apart). These non-stringent restarting ART criteria were chosen to avoid missing a potential control of HIV-1 replication after a potential peak of viremia after ATI. Participants who reached week 48 of follow-up without meeting restart criteria were advised to restart ART if they had detectable plasma viremia (>20 HIV-1 RNA copies/ml).

The safety end point was the proportion of participants with vedolizumab treatment-related adverse events and its severity. All adverse events, severity and relationship to study product during vedolizumab infusion and follow-up were reported according to

the Division of AIDS Table for Grading the Severity of Adult and Pediatric Adverse Events, version 2.0, November 2014. The virological endpoint was defined as the number of participants remaining off ART and who achieved undetectable viral load at week 48 according to the criteria above mentioned.

For post-hoc efficacy analysis we compared this group of participants (vedolizumab group) with historical controls matched by age, sex and time of infection, corresponding to the placebo arm of the AELIX-002 (NCT03204617) vaccine trial performed in early-treated PLWH that also included an ATI (28) for 24 weeks using the same ART resumption criteria than the vedolizumab group.

Laboratory methods

Absolute CD4^{+} and CD8^{+} T-cell counts were measured using an FC500 Flow Cytometer (Beckman-Coulter). The plasma HIV-1 RNA concentration was measured by quantitative polymerase chain reaction (COBAS Ampliprep/COBAS Taqman HIV-1 Test, Roche Molecular Systems; lower detection limit of 20 HIV-1 RNA copies/mL) according to the manufacturer's protocol.

Peripheral blood mononuclear cells isolation

Peripheral blood mononuclear cells (PBMCs) were isolated using BD Vacutainer CPT Mononuclear Cell Preparation Tubes (with Sodium Heparin) by density gradient centrifugation one week before each vedolizumab infusion before ATI and at weeks 28, 32, 36, 40, 44 and 48 of follow-up. PBMCs were cryopreserved in liquid nitrogen until further use.

Isolation of gastrointestinal (GI) cells

Ileal and cecal biopsies were obtained during colonoscopy at BL and at ATI start (week 24). These two locations were biopsied for having a representation of immune inductive and effector sites, respectively (66). Fresh biopsies (10-13 pieces) were transported in R10 medium (RPMI medium supplemented with 10 % FBS, 1% penicillin and 1% L-glutamine) and processed immediately. Intestinal biopsies were washed with phosphate buffered saline (PBS) and 14% ethylene diamine tetra-acetic acid (EDTA) during 30 minutes at 37°C in agitation. The biopsies were then physically disrupted with blades.

531   Next, the intestinal biopsies were transferred to 20 ml of R10 containing 20 mg of Type
532   IV collagenase (Sigma-Aldrich) and incubated for 30 minutes at 37°C with gentle
533   agitation. After the first 15 minutes round of incubation with collagenase solution,
534   biopsies were physically disrupted by syringes with needles. The disrupted tissue was
535   transferred into the R10-collagenase solution for a second round of 15 minutes
536   incubation in gentle agitation. After incubation, single-cell suspension was obtained by
537   filtering through a 70 μm cell strainer and washed with R10 medium. Cells were
538   cryopreserved in liquid nitrogen until further use. Two biopsies' pieces were frozen
539   intact in RNA-later and snap frozen at -80°C for further RNA and DNA extraction.

540

541   **Assay of soluble biomarkers and plasma levels of retinoic acid**
542   Serum and plasma samples were collected in serum separation tubes and in EDTA tubes
543   and stored at -20°C until subsequent analysis of the following biomarkers: high-
544   sensitivity C-reactive protein (hsCRP), β2-microglobulin (β2M) and D-dimer (DD). The
545   levels of hsCRP and β2M were determined by an immunoturbidimetric serum assay
546   using a Cobas 701 analyzer (Roche Diagnostics). DD levels were measured by an
547   automated latex-enhanced immunoassay (HemosIL D-dimer HS 500; Instrumentation
548   Laboratory). Retinoic acid plasma levels were determined by UHPLC-MS/MS according
549   to previously described method (67–69). All the assays were performed following the
550   manufacturers' instructions.

551

552   **Plasma levels of vedolizumab and immunogenicity**
553   Serum concentrations of vedolizumab and the presence of antidrug antibodies (ADAs)
554   were determined in serum samples using the enzyme-linked immunosorbent assay
555   (ELISA) RIDASCREE VDZ Monitoring (r-biopharm). The assays were performed following
556   the manufacturer's instructions.

557

558   **Immunophenotyping and quantification of α4β7 cells**
559   *Cryopreserved PBMCs* were thawed, washed (1800 rpm, 5min, room temperature) with
560   phosphate-buffered saline (PBS) and incubated 35 min at room temperature with
561   LIVE/DEAD Fixable Aqua Dead Cell Stain (Life Technologies) and extracellular anti-human
562   antibodies anti-CD45RA (FITC); anti-TIGIT (PerCP-Cy5.5); anti-LAG3 (BV605); anti-PD1

563 (BV510); anti-integrin β7 (BV711); anti-CD27 (BV786); anti-CD38 (BV650); anti-CD3

564 (APCH7); anti-integrin α4β7 (APC); anti-TIM3 (PeCF594); anti-HLA-DR (BV570); anti-CD4

565 (AF 700); anti-CD19, anti-CD14 and anti-CD56 (Pacific Blue) (See supplementary table 3).

566 PBMCs were then washed with PBS and permeabilized with Fixation/Permeabilization

567 FoxP3 Kit (eBioscience) according to the manufacturer's instructions. Cells were stained

568 intracellularly at 4°C for 30min with anti-Ki67 (PE), and then washed and fixed in PBS

569 containing 4% paraformaldehyde (PFA). Samples were acquired using LSR-II Fortessa

570 Cytometer (BD Immunocytometry Systems) and analyses were performed using FlowJo,

571 version 9.2.

572

573 *Isolated GI cells* were thawed, washed (1800 rpm, 5min, room temperature) with PBS

574 and incubated 35 min at room temperature with LIVE/DEAD fixable Violet Dead cell stain

575 and extracellular anti-human antibodies anti-CCR6 (AF 647); anti-CD45RA (FITC); anti-

576 CD25 (PE-Cy7); anti-CXCR5 (BV421); anti-LAG3 (BV605); anti-CXCR3 (PerCP-Cy5.5); anti-

577 PD1 (BV510); anti-CD127 (BUV737); anti-CD45 (BUV805); anti-CD8 (BUV615); anti-CD69

578 (BB700); anti-CD103 (BV480); anti-CCR7 (BUV563); anti-CD3 (APC-H7); anti-TIM3

579 (PE/DAZZLE 594); anti-integrin α4β7 (APC); anti-CD123 (Alexa Fluor700); anti-CD11c

580 (BV650); anti-HLA-DR (BV570); anti-integrin β7 (BV711); anti-CD27 (BV786); anti-CD19,

581 anti-CD14, anti-CD20 and anti-CD56 (Pacific Blue) (See Supplementary table 3). Cells

582 were then washed and permeabilized using Fixation/Permeabilization FoxP3 Kit

583 (eBioscience) according to the manufacturer's instructions. Cells were stained

584 intracellularly at 4°C for 30min with anti-FoxP3 (PE-Cy5) and anti-Ki67 (PerCP-eFluor

585 710) and then washed and fixed in PBS containing 4% paraformaldehyde (PFA). Samples

586 were acquired using Cytek Aurora Spectral Cytometer 4L (Cytek Biosciences) and

587 analyses were performed using FlowJo, version 9.2.

588

589 Anti-integrin α4β7 mAb (APC; clone: ACT-1) was kindly provided by Dr. Danlan Wei and

590 Dr. James Arthos, National Institute of Allergy and Infectious Disease (NIAID-NIH,

591 Bethesda, Maryland, USA). Anti-integrin α4β7 mAb (APC; clone: ACT-1) and vedolizumab

592 share the same epitope. Quantification of integrin α4β7 levels was performed using anti-

593 α4β7 mAb (APC; clone: ACT-1) at BL and by gating CD4+CD45RO+β7+ along the follow-

594 up. Previous studies have demonstrated that CD4+CD45RO+β7+ cells in peripheral blood

595   are >99% α4β7+ (9, 14, 31, 32); therefore, this gating strategy was used to quantify α4β7

596   expression on CD4+ T-cells (Supplementary Fig. 9). The percentage of α4β7 integrin

597   blocked by vedolizumab was calculated through the combination of anti-α4β7 (APC;

598   clone: ACT-1) and anti-β7 (BV711; clone: FIB504).

599

Cell sorting

601   CD4 memory T-cells α4β7+ and α4β7- were sorted from PBMCs. Cryopreserved PBMCs

602   were thawed, washed with PBS (1800 rpm, 5min, room temperature) and incubated 35

603   min at room temperature with LIVE/DEAD Fixable Violet Dead cell stain and extracellular

604   anti-human antibodies anti-CD45RA (FITC); anti-integrin β7 (BV711); anti-integrin α4β7

605   (APC); anti-CD27 (BV786); anti-CD3 (APC-H7); anti-CD4 (AF700); anti-CD19, anti-CD14

606   and anti-CD56 (Pacific Blue) (See supplementary Table 3). CD4+CD45RO+β7+ and

607   CD4+CD45RO+β7- cells were sorted using BD FACSAria Fusion Flow Cytometer (BD

608   Immunocytometry Systems) and analysis was performed using FlowJo, version 9.2.

609

Quantitation of cell-associated HIV-1 DNA and RNA

611   The procedures for quantitation of total cell-associated HIV-1 DNA and RNA have been

612   previously described in detail (70). Briefly, levels of total cell-associated HIV-1 DNA and

613   RNA were quantified by droplet digital PCR (ddPCR) from extracted DNA and RNA using

614   the BIO-RAD QX200 Droplet Reader. Genomic DNA was extracted using Blood DNA Mini

615   Kit (Omega, Bio-Tek) for the bulk of PBMCs and QIAamp DNA Micro Kit (Qiagen) for

616   CD4+CD45RO+ β7+ and β7- sorted cells following the manufacturer's protocol. RNA was

617   extracted using NucleoSpin RNA purification kit (Macherey-Nagel) for the bulk of PBMCs

618   and RNeasy Micro Kit (Qiagen) for sorted cells following the manufacturer's protocol.

619   DNA and RNA concentration were measured by the Qubit Assay (ThermoFisher

620   Scientific) and carried to 30 ng/μL concentration. Bio-Rad QX200 ddPCR system was run

621   according to the manufacturer's protocol, using an annealing temperature of 58°C, using

622   two pair of primers targeting LTR and Gag regions (70). Copy numbers were calculated

623   using Bio-Rad QuantaSoft software v.1.7.4. RPP30 (to cell-associated HIV-1 DNA) and

624   TBP genes (to cell-associated HIV-1 RNA) were the host cell genes used to normalize HIV-

625   1 copies.

626

Full-Length Individual Proviral Sequencing (FLIP-seq) in PBMCs

FLIP-seq was assayed in PBMCs at week 24. Genomic DNA, previously extracted from PBMCs (DNeasy Blood & Tissue kit, QIAGEN), was diluted to single proviral genomes based on ddPCR results and Poisson distribution statistics, where one provirus was present in approximately 20-30% of wells. Subsequently, DNA was subjected to HIV-1 near-full-genome amplification using a single-amplicon nested PCR approach. The reaction was composed of: one unit of Invitrogen Platinum Taq (catalog 11302-029) per 20 μl of reaction, 1x reaction buffer, 2 mM $MgSO_4$, 0.2 mM dNTP, and 0.4 μM of forward (first-round nested-PCR: U5-623F, 5'-AAATCTCTAGCAGTGGCGCCCGAACAG-3'; second-round nested-PCR: U5-638F, 5'-GCGCCCGAACAGGGACYTGAAARCGAAAG-3') and reverse primer (first-round nested-PCR: U5-601R, 5'-TGAGGGATCTCTAGTTACCAGAGTC-3'; second-round nested-PCR: U5-547R, 5'-GCACTCAAGGCAAGCTTTATTGAGGCTTA-3'). The PCR was performed using the following thermocycler program: 2 min at 92 °C, 10 cycles [10 s at 92 °C, 30 s at 60 °C, 10 min at 68 °C], 20 cycles [10 s at 92 °C, 30 s at 55 °C, 10 min at 68 °C], 10 min at 68 °C and 4 °C infinite hold. PCR products were visualized by agarose gel electrophoresis. All near full-length were subjected to Illumina MiSeq sequencing at the MGH DNA Core facility. Large deleterious deletions (<8000 bp of the amplicon aligned to HXB2), out-of-frame indels, premature/lethal stop codons, internal inversions, or packaging signal deletions (≥15 bp insertions and/or deletions relative to HXB2) were identified by an automated pipeline written in Python programming language (https://github.com/BWH-Lichterfeld-Lab/Intactness-Pipeline)(71) and the presence/absence of APOBEC-3G/3F-associated hypermutations was determined using Los Alamos National Laboratory (LANL) HIV-1 Sequence Database Hypermut 2.0 program (72). Viral sequences without any of the mutations previously mentioned were classified as intact sequences. Phylogenetic distances between sequences were determined through maximum-likelihood trees in MEGA (https://www.megasoftware.net/) and visualized with Highlighter plots (https://www.HIV-1.lanl.gov/content/sequence/HIGHLIGHT/highlighter_top.html).

Statistical analysis

658 Continuous variables were expressed as medians and interquartile ranges (IQRs), and

659 categorical variables were expressed as numbers and percentages. Friedman Test with

660 Dunn's multiple comparisons test correction was used to assess differences along the

661 follow-up. The Wilcoxon signed-rank test was used to analyze related samples and

662 Mann-Whitney U and Chi-square tests were used to analyze differences between

663 groups. Correlations between variables were assessed using Spearman's rank test. Log

664 rank test and Kaplan-Meier curves were used for time to event analysis regarding

665 virological efficacy compared to historical control group. All p values <0.05 were

666 considered significant. Statistical analysis was performed using Statistical Package for

667 the Social Sciences software (SPSS 22.0; SPSS, Chicago, IL, USA). Multiple immune

668 checkpoint phenotype were constructed using Pestle version 1.6.2 and Spice version 6

669 (provided by M. Roederer, NIH, Bethesda, MD) and quantified with the polyfunctionality

670 index algorithm (Pindex) employing the 0.1.2 beta version of FunkyCells Boolean

671 Dataminer software, provided by Martin Larson (INSERM U1135, Paris, France) as

672 previously described (73).

673

674 **Study approval**

675 All participants gave written informed consent prior to study start; and the clinical trial

676 was approved by the Seville Provincial Ethics Committee of research with medicines

677 (NCT03577782, please visit https://clinicaltrials.gov/ for protocol summary; Internal

678 Code: FIS-VED-2017-01, Study Code: Nº EudraCT: 2018-000497-30) and authorized by

679 the Spanish Agency for Medicines and Medical Devices (AEMPS).

680

681 **Data availability.**

682 Due to the sensitivity of the data, individual participant data will not be made available.

683 Data generated by this study are available in the "Supporting data values" XLS file or

684 upon request to the corresponding author.

685

686 **AUTHOR CONTRIBUTIONS**

687 All authors reviewed and approved the submitted version of the manuscript. MRJL and

688 CGC contributed equally to this work. LLC, PV, NE and CRO recruited the participants and

689 provided PLWH blood samples. IRJ, AJCB and RM supervised the clinical trial. S.S and

24

690 MFA performed de biopsies and provided PLWH GITs samples. ERM, MRJL and CGC

691 designed the experiments. MRJL, CGC, CG, IR, GG, JGSH, RRB, FG and AIAR performed

692 the experiments. MRJL, CGC and ERM analyzed, interpreted the data and wrote of the

693 paper. JV, SB, APG, XY and ML reviewed and contributed to paper discussion. ERM,

694 conceived the idea, coordinated the project and acquired funding for the study.

695

712

713

REFERENCES

714

715 1. Finzi D, et al. Identification of a Reservoir for HIV-1 in Patients on Highly Active Antiretroviral
716 Therapy. *Science (1979)*. 1997;278:1295–1300.

717 2. Martin HA, et al. New Assay Reveals Vast Excess of Defective over Intact HIV-1 Transcripts in
718 Antiretroviral Therapy-Suppressed Individuals. *J Virol*. 2022;96(24):e0160522.

719 3. Richman DD, et al. The challenge of finding a cure for HIV infection. *Science*.
720 2009;323(5919):1304–1307.

721 4. Chun TW, et al. Presence of an inducible HIV-1 latent reservoir during highly active
722 antiretroviral therapy. *Proc Natl Acad Sci U S A*. 1997;94(24):13193–13197.

723 5. Siliciano JD, et al. Long-term follow-up studies confirm the stability of the latent reservoir for
724 HIV-1 in resting CD4+ T cells. *Nat Med*. 2003;9(6):727–728.

725 6. Montaner JSG, et al. Rebound of plasma HIV viral load following prolonged suppression with
726 combination therapy. *AIDS*. 1998;12(11):1398–1399.

727 7. Pernas M, et al. Factors Leading to the Loss of Natural Elite Control of HIV-1 Infection. *J Virol*.
728 2018;92(5):e01805-17.

729 8. Mehandru S, Dandekar S. Role of the gastrointestinal tract in establishing infection in
730 primates and humans. *Curr Opin HIV AIDS*. 2008;3(1):22–27.

731 9. Cicala C, et al. The integrin alpha4beta7 forms a complex with cell-surface CD4 and defines a
732 T-cell subset that is highly susceptible to infection by HIV-1. *Proceedings of the National*
733 *Academy of Sciences*. 2009;106(49):20877–20882.

734 10. Erle DJ, et al. Expression and function of the MAdCAM-1 receptor, integrin alpha 4 beta 7,
735 on human leukocytes. *The Journal of Immunology*. 1994;153(2):517–28.

736 11. Guzzo C, et al. Virion incorporation of integrin $\alpha 4\beta 7$ facilitates HIV-1 infection and
737 intestinal homing. *Sci Immunol*. 2017;2(11):1–30.

738 12. Arthos J, et al. HIV-1 envelope protein binds to and signals through integrin $\alpha 4\beta 7$, the gut
739 mucosal homing receptor for peripheral T cells. *Nat Immunol*. 2008;9(3):301–309.

740 13. Kader M, et al. $\alpha 4+\beta 7$hiCD4+ memory T cells harbor most Th-17 cells and are preferentially
741 infected during acute SIV infection. *Mucosal Immunol*. 2009;2(5):439–449.

742 14. Sivro A, et al. Integrin $\alpha 4\beta 7$ expression on systemic CD4+ T cells predicts higher rates of HIV
743 acquisition and disease progression. *Sci Transl Med*. 2018;10:1–10.

744 15. Martinelli E, et al. The frequency of $\alpha_4\beta_7$(high) memory CD4$^+$ T cells correlates with
745 susceptibility to rectal simian immunodeficiency virus infection. *J Acquir Immune Defic Syndr*.
746 2013;64(4):325–331.

747 16. Byrareddy SN, et al. Species-specific differences in the expression and regulation of $\alpha 4\beta 7$
748 integrin in various nonhuman primates. *J Immunol*. 2015;194(12):5968–5979.

749 17. Ansari AA, et al. Blocking of α4β7 Gut-Homing Integrin during Acute Infection Leads to
750 Decreased Plasma and Gastrointestinal Tissue Viral Loads in Simian Immunodeficiency Virus-
751 Infected Rhesus Macaques. *The Journal of Immunology*. 2011;186(2):1044–1059.

752 18. Byrareddy SN, et al. Targeting α4β7 integrin reduces mucosal transmission of simian
753 immunodeficiency virus and protects gut-associated lymphoid tissue from infection. *Nat Med*.
754 2014;20(12):1397–1400.

755 19. Byrareddy SN, et al. Sustained virologic control in SIV+ macaques after antiretroviral and
756 alpha4beta7 antibody therapy. *Science (1979)*. 2016;354(6309):197–202.

757 20. Feagan BG, et al. Vedolizumab as Induction and Maintenance Therapy for Ulcerative Colitis.
758 *N Engl J Med*. 2013;8(8):699–710.

759 21. Sandborn WJ, et al. Vedolizumab as Induction and Maintenance Therapy for Crohn's
760 Disease. *N Engl J Med*. 2013;369(8):711–732.

761 22. Soler D, et al. The Binding Specificity and Selective Antagonism of Vedolizumab, an Anti-
762 α4β7 Integrin Therapeutic Antibody in Development for Inflammatory Bowel Diseases. *Journal
763 of Pharmacology and Experimental Therapeutics*. 2009;330(3):864–875.

764 23. Sneller MC, et al. An open-label phase 1 clinical trial of the anti-α4β7 monoclonal antibody
765 vedolizumab in HIV-infected individuals. *Sci Transl Med*. 2019;11(509):1–9.

766 24. Iwamoto N, et al. Blocking alpha4beta7 integrin binding to SIV does not improve virologic
767 control. *Science (1979)*. 2019;365(6457):1033–1036.

768 25. Di Mascio M, et al. Evaluation of an antibody to alpha4beta7 in the control of SIVmac239-
769 nef-stop infection. *Science (1979)*. 2019;365:1025–1029.

770 26. Abbink P, et al. Lack of therapeutic efficacy of an antibody to alpha4beta7 in SIVmac251-
771 infected rhesus macaques. *Science (1979)*. 2019;365(6457):1029–1033.

772 27. Fromentin R, et al. CD4+ T Cells Expressing PD-1, TIGIT and LAG-3 Contribute to HIV
773 Persistence during ART. *PLoS Pathog*. 2016;12(7):e1005761.

774 28. Bailón L, et al. Safety, immunogenicity and effect on viral rebound of HTI vaccines in early
775 treated HIV-1 infection: a randomized, placebo-controlled phase 1 trial. *Nat Med*.
776 2022;28(12):2611–2621.

777 29. Fellay J, et al. A Whole-Genome Association Study of Major Determinants for Host Control
778 of HIV-1. *Science (1979)*. 2007;317(5840):944–947.

779 30. Pereyra F. The Major Genetic Determinants of HIV-1 Control Affect HLA Class I Peptide
780 Presentation. *Science*. 2010;330(6010):1551–1557.

781 31. Martin AR, et al. The association of α4β7 expression with HIV acquisition and disease
782 progression in people who inject drugs and men who have sex with men: Case control studies.
783 *EBioMedicine*. 2020;62:103102 (1–7).

784   32. Wang X, et al. Monitoring alpha4beta7 integrin expression on circulating CD4+ T cells as a
785   surrogate marker for tracking intestinal CD4+ T-cell loss in SIV infection. *Mucosal Immunol*.
786   2009;2(6):518–526.

787   33. Cicala C, Arthos J, Fauci AS. Role of T-cell trafficking in the pathogenesis of HIV disease. *Curr*
788   *Opin HIV AIDS*. 2019;14(2):115–120.

789   34. Sidell N, Kane MA. Actions of Retinoic Acid in the Pathophysiology of HIV Infection.
790   *Nutrients*. 2022;12;14(8):1. https://doi.org/10.3390/nu14081611.

791   35. Li JZ, et al. The Size of the Expressed HIV Reservoir Predicts Timing of Viral Rebound after
792   Treatment Interruption. *AIDS*. 2016;30(3):343–53.

793   36. Martin GE, et al. Post-treatment control or treated controllers? Viral remission in treated
794   and untreated primary HIV infection. *AIDS*. 2017;31:477–484.

795   37. Massanella M, et al. Long-term effects of early antiretroviral initiation on HIV reservoir
796   markers: a longitudinal analysis of the MERLIN clinical study. *Lancet Microbe*. 2021;2(5):e198–
797   e209.

798   38. Besson GJ, et al. HIV-1 DNA Decay Dynamics in Blood During More Than a Decade of
799   Suppressive Antiretroviral Therapy. *Clinical Infectious Diseases*. 2014;59(9):1312–1321.

800   39. Viard JP, et al. Impact of 5 years of maximally successful highly active antiretroviral therapy
801   on CD4 cell count and HIV-1 DNA level. *Aids*. 2004;18(1):45–49.

802   40. Tincati C, et al. Early initiation of highly active antiretroviral therapy fails to reverse
803   immunovirological abnormalities in gut-associated lymphoid tissue induved by acute HIV
804   infection. *Antivir Ther*. 2009;14:321–330.

805   41. Chintanaphol M, et al. Feasibility and safety of research sigmoid colon biopsy in a cohort of
806   Thai men who have sex with men with acute HIV-1. *J Virus Erad*. 2020;6(1):7–10.

807   42. Honeycutt JB, et al. Macrophages sustain HIV replication in vivo independently of T cells. *J*
808   *Clin Invest*. 2016;126(4):1353–1366.

809   43. Thornhill JP, et al. Vedolizumab use and the associations between alpha4beta7 expression
810   and HIV reservoir in the gut during treated primary HIV infection. *Aids*. 2019;33(14):2266–
811   2268.

812   44. Fisher K, et al. Plasma-Derived HIV-1 Virions Contain Considerable Levels of Defective
813   Genomes. *J Virol*. 2022;96(6):e0201121.

814   45. Joag VR, et al. Identification of preferential CD4+ T-cell targets for HIV infection in the
815   cervix. *Mucosal Immunol*. 2016;9:1–12.

816   46. Cicala C, Arthos J, Fauci AS. HIV-1 envelope, integrins and co-receptor use in mucosal
817   transmission of HIV. *J Transl Med*. 2010;9(S1:S2):1–10.

818   47. Dufour C, et al. Phenotypic characterization of single CD4+ T cells harboring genetically
819   intact and inducible HIV genomes. *Nat Commun*. 2023;14(1):1115.

820   48. Rindi LV, et al. Drug-Induced Progressive Multifocal Leukoencephalopathy (PML): A
821   Systematic Review and Meta-Analysis. *Drug Saf*. [published online ahead of print: February 7,
822   2024]. https://doi.org/10.1007/s40264-023-01383-4.

823   49. Loftus E V., et al. Long-term safety of vedolizumab for inflammatory bowel disease. *Aliment*
824   *Pharmacol Ther*. 2020;52(8):1353–1365.

825   50. Pereira LE, et al. Preliminary in vivo efficacy studies of a recombinant rhesus anti-α4β7
826   monoclonal antibody. *Cell Immunol*. 2009;259(2):165–176.

827   51. Frank I, et al. Blocking α4β7 integrin delays viral rebound in SHIVSF162P3-infected
828   macaques treated with anti-HIV broadly neutralizing antibodies. *Sci Transl Med*.
829   2021;13(607):1–13.

830   52. Sun Y, Xue J. Expression Profile and Biological Role of Immune Checkpoints in Disease
831   Progression of HIV/SIV Infection. *Viruses*. 2022;14(581):1–28.

832   53. Hurst J, et al. Immunological biomarkers predict HIV-1 viral rebound after treatment
833   interruption. *Nat Commun*. 2015;6:8495 (1–9).

834   54. Imamichia H, et al. Defective HIV-1 proviruses produce novel protein-coding RNA species in
835   HIV-infected patients on combination antiretroviral therapy. *Proc Natl Acad Sci U S A*.
836   2016;113(31):8783–8788.

837   55. Goode D, et al. HSV-2-driven increase in the expression of α4β7 correlates with increased
838   susceptibility to vaginal SHIV(SF162P3) infection. *PLoS Pathog*. 2014;10(12):e1004567.

839   56. Cicala C, Arthos J, Fauci AS. Role of T-cell trafficking in the pathogenesis of HIV disease. *Curr*
840   *Opin HIV AIDS*. 2019;14(2):115–120.

841   57. Perreau M, et al. Follicular helper T cells serve as the major CD4 T cell compartment for
842   HIV-1 infection, replication, and production. *Journal of Experimental Medicine*.
843   2013;210(1):143–156.

844   58. Renault C, et al. Th17 CD4+ T-Cell as a Preferential Target for HIV Reservoirs. *Front*
845   *Immunol*. 2022;13:1–14.

846   59. Kanwar B, Favre D, McCune JM. Th17 and regulatory T cells: Implications for AIDS
847   pathogenesis. *Curr Opin HIV AIDS*. 2010;5(2):151–157.

848   60. Iwata M, et al. Retinoic acid imprints gut-homing specificity on T cells. *Immunity*.
849   2004;21(4):527–538.

850   61. Ross AC. Vitamin A and retinoic acid in T cell-related immunity. *Am J Clin Nutr*.
851   2012;96(5):1166S–72S.

852   62. Mora JR, Iwata M, Von Andrian UH. Vitamin effects on the immune system: vitamins A and
853   D take centre stage. *Nat Rev Immunol*. 2008;8:685–697.

854   63. Nawaz F, et al. MAdCAM costimulation through Integrin-α 4 β 7 promotes HIV replication.
855   *Mucosal Immunol*. 2018;11(5):1342–1351.

856   64. Kaiser P, et al. Stimulating the RIG-I pathway to kill cells in the latent HIV reservoir
857   following viral reactivation. *Nat Med*. 2016;22:807–811.

858   65. Uzzan M, et al. Anti-α4β7 therapy targets lymphoid aggregates in the gastrointestinal tract
859   of HIV-1–infected individuals. *Sci Transl Med*. 2018;10(461):eaau4711.

860   66. Mowat A. M.; Viney J. L. The anatomical basis of intestinal immunity. *Immunol Rev*.
861   1997;156:145–166.

862   67. Gundersen TE, Bastani NE, Blomhoff R. Quantitative high-throughput determination of
863   endogenous retinoids in human plasma using triple-stage liquid chromatography/tandem mass
864   spectrometry. *Rapid Communications in Mass Spectrometry*. 2007;21(7):1176–1186.

865   68. Saha A, et al. High Throughput LC-MS/MS Method for Simultaneous Estimation of 9-Cis-
866   Retinoic Acid and its Metabolite 4-Oxo-9-Cis-Retinoic Acid in Human Plasma and its Application
867   to a Bioequivalence Study. *J Anal Bioanal Tech*. 2015;6(13):1–18.

868   69. Arnold SLM, et al. A sensitive and specific method for measurement of multiple retinoids in
869   human serum with UHPLC-MS/MS. *J Lipid Res*. 2012;53(3):587–598.

870   70. de Pablo-Bernal RS, et al. Modulation of Monocyte Activation and Function during Direct
871   Antiviral Agent Treatment in Patients Coinfected with HIV and Hepatitis C Virus. *Antimicrob
872   Agents Chemother*. 2020;64(9):1–13.

873   71. Lee GQ, et al. HIV-1 DNA sequence diversity and evolution during acute subtype C
874   infection. *Nat Commun*. 2019;10:2737 (1–11).

875   72. Rose PP, Korber BT. Detecting hypermutations in viral sequences with an emphasis on G →
876   A hypermutation. *Bioinformatics*. 2000;16(4):400–401.

877   73. Dominguez-Molina B, et al. Immune Correlates of Natural HIV Elite Control and
878   Simultaneous HCV Clearance-Supercontrollers. *Front Immunol*. 2018;9 (2897):1–13.

879

880

965 **Table 1. Characteristics of study participants.**

Characteristic	Vedolizumab group (n=10)	Historical Control group[a] (n=15)	*p* value
Age (years) at study entry	39.8 [27.0 – 42.6]	34.0 [30.0 – 42.0]	0.657
Male sex (%)	90	100	0.211
Time since HIV infection at study entry (days)	75 [40 – 82]	55 [30 – 108]	0.912
CD4+ T-cell counts (cells/mm^3) at study entry	540 [401 – 735]	826 [608 – 950]	**0.006**
CD8+ T-cell counts (cells/mm^3) at study entry	1093 [603 – 1287]	937 [468 – 1101]	0.202
Ratio CD4+/CD8+ T-cells at study entry	0.5 [0.4 – 0.9]	1.1 [0.7 – 1.6]	**0.011**
Pre ART viral load (Log$_{10}$ HIV-1-RNA copies/mL)	5.7 [5.0 – 6.9]	4.9 [4.4 – 5.9]	0.101
Time on ART at ATI[b] start (years)	0.5 [0.5 – 0.5]	1.9 [1.6 – 3.2]	**<0.0001**
Time with undetectable viral load at ATI start (years)	0.3 [0.3 – 0.4]	1.5 [1.3 – 2.9]	**<0.0001**
INSTI based ART, n (%)	10 (100)	15 (100)	>0.999

966 Continuous variables were expressed as medians and interquartile ranges (IQRs), and
967 categorical variables were expressed as numbers and percentages. The Mann-Whitney U and
968 Chi-square tests were used to analyze differences of continuous and categorical variables
969 between groups, respectively.

970 [a]Historical participants in the placebo arm of a therapeutic vaccine trial [27].

971 [b]Antiretroviral treatment interruption.

972

34
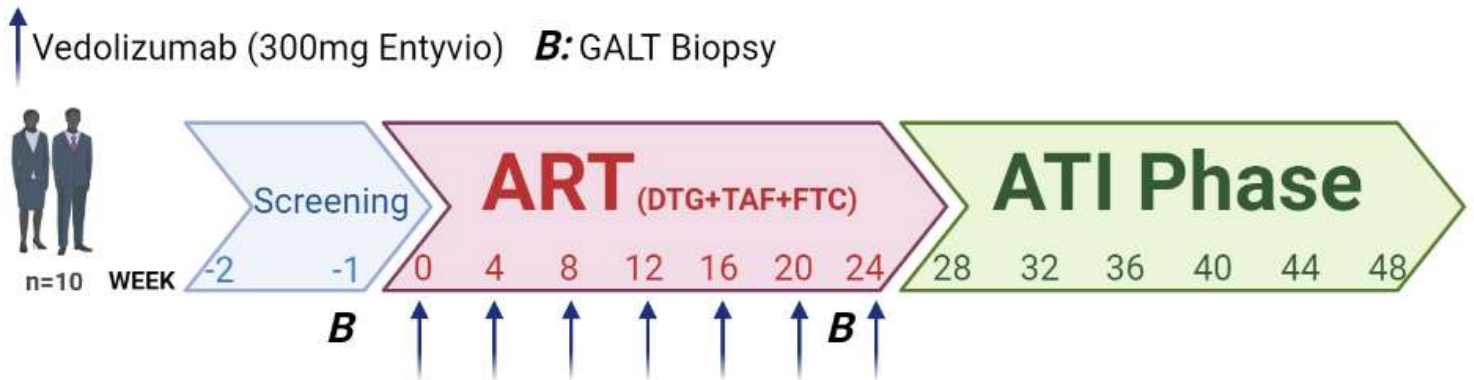
Fig. 1. Clinical trial design. Ten individuals with HIV-1 diagnosis in acute/recent infection phase were enrolled. Participants started ART together with vedolizumab infusions (300 mg) at week 0, 4, 8, 12, 16, 20 and 24. At week 24, ART and vedolizumab treatment were interrupted. Biopsies were obtained from ileum and caecum at week 0 and 24. Abbreviations: GALT, gut-associated lymphoid tissue; ART, antiretroviral therapy and ATI, analytic treatment interruption. Figure created with Biorender.com
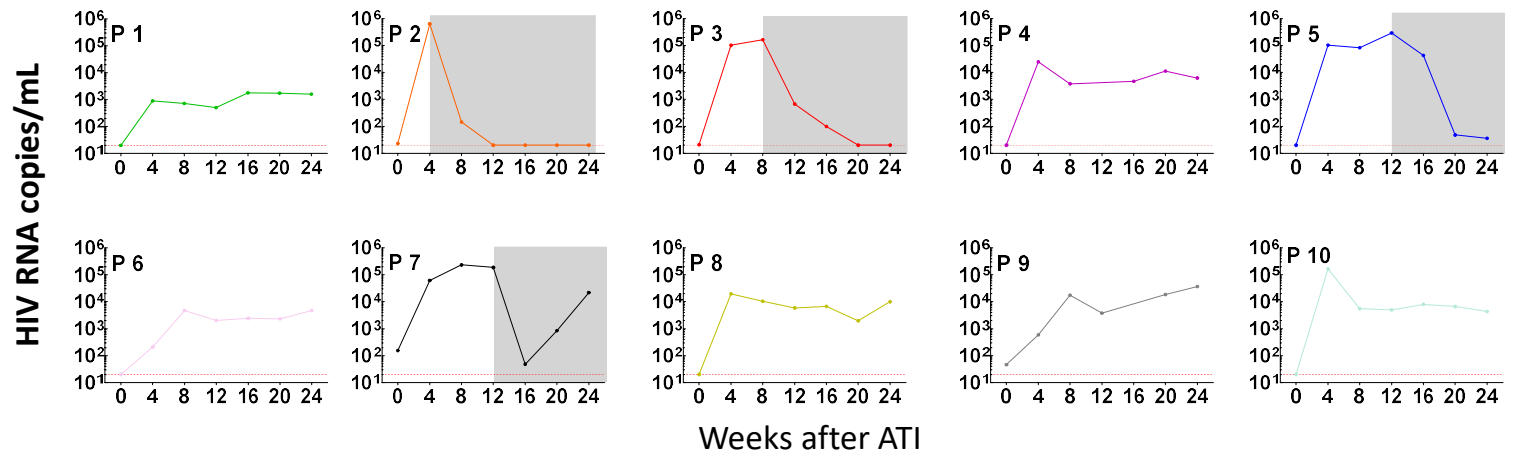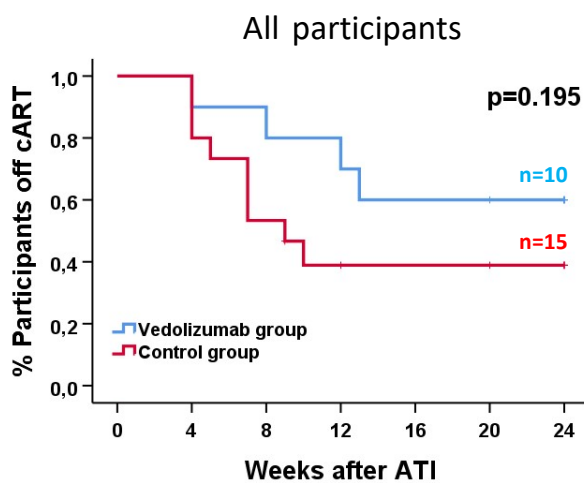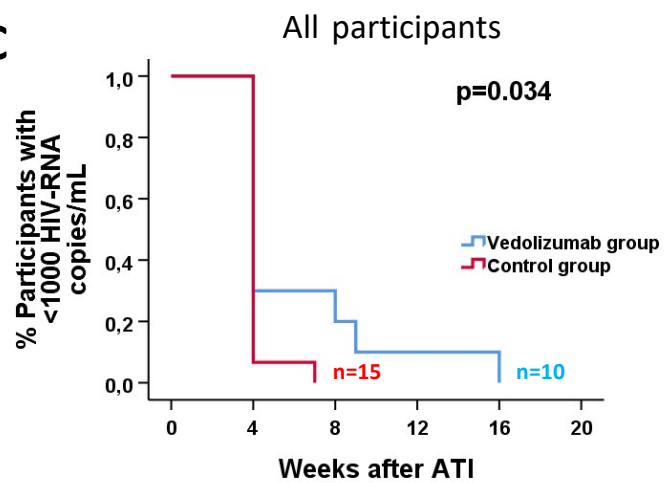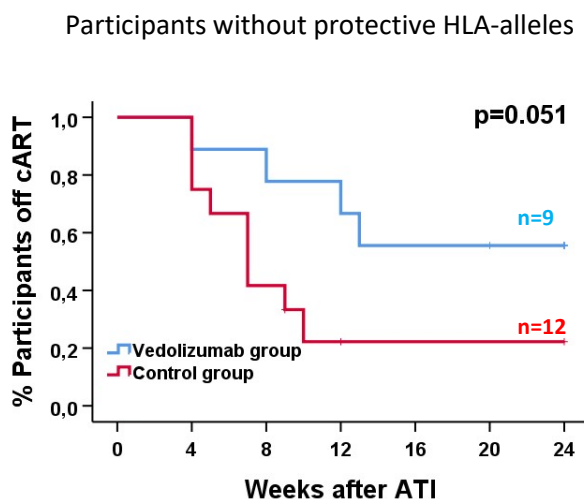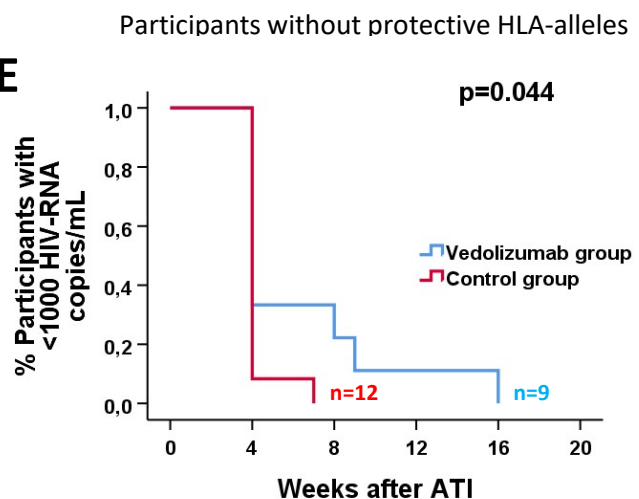
Fig. 2. Plasma viral load, proportion of participants off ART and time to viral load rebound after ATI. (a) Longitudinal plasma viremia evolution after ATI. Four participants restarted ART (grey area) due to an increase of viral load (>10^5 HIV-1-RNA copies/ml). Horizontal red line indicates the limit of detection (20 HIV-RNA copies/ml). **(b)** Kaplan-Meier analysis of the proportion of participant off ART after ATI compared to historical control group. **(c)** Kaplan-Meier analysis between vedolizumab and historical control group of the time to first VL>1000 HIV-RNA copies/ml. **(d-e)** Kaplan-Meier analysis considering only participants without protective alleles (HLA-B*27 and HLA-B*57). In this analysis, participants 36, 16 and 17 from historical control cohort and participant 4 from the vedolizumab group were excluded. Wilcoxon test, log rank and Kaplan-Meier curves were used to assess differences along the follow-up. Abbreviations: BL, baseline; W, week; and ATI, analytic treatment interruption.
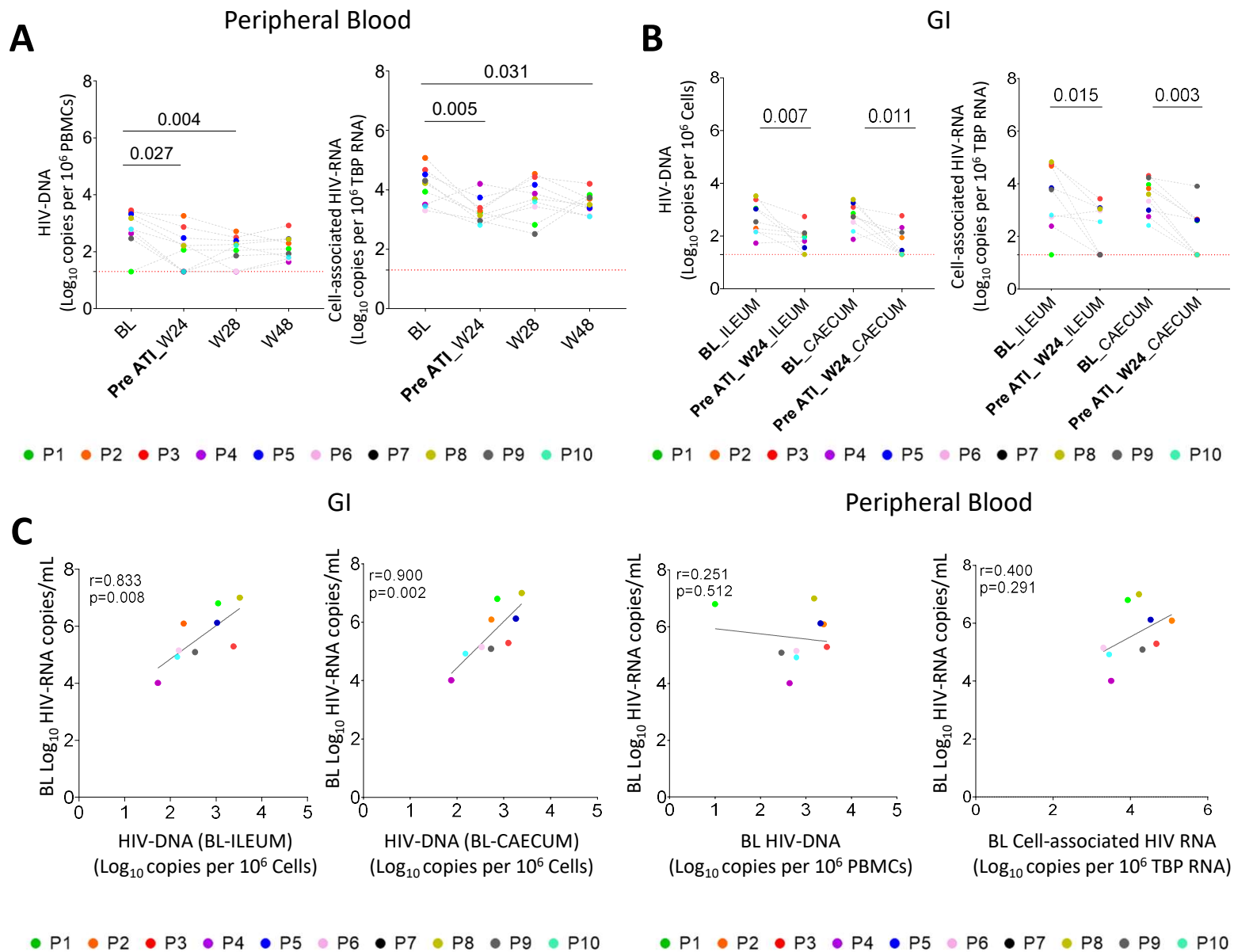
Fig. 3. Dynamics of HIV-1 reservoir. (a) Total cell-associated HIV-1-DNA and RNA in PBMCs along the follow-up. **(b)** Cell-associated HIV-1-DNA and RNA in ileum and caecum cells at BL and week 24. **(c)** Associations between HIV-1 reservoir in GITs (cell associated HIV-DNA) and PBMCs (cell associated HIV-DNA and RNA) and plasma viral load at BL. Horizontal red line indicates the limit of detection. Friedman test with Dunn's multiple comparisons test correction was used to assess differences along the follow-up and Mann-Whitney U test between GIT locations. Abbreviations: BL, baseline; W, week; and ATI, analytic treatment interruption.
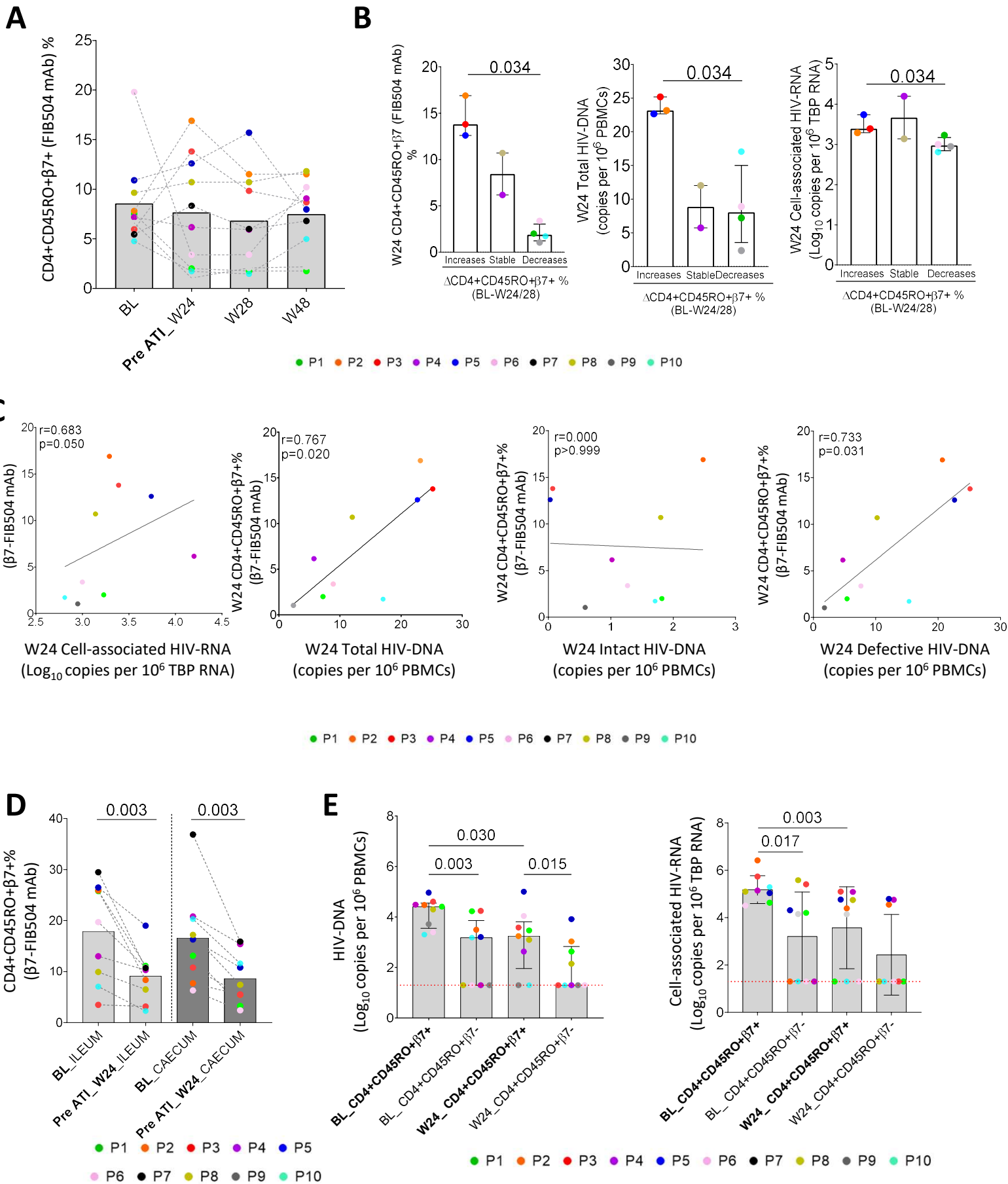
Fig. 4. Analysis of the dynamic of β7 expression levels and association with the size of the HIV-1 reservoir at week 24. (a) Dynamic of α4β7 expression on CD4 T-cells along the follow-up in PBMCs. **(b)** Correlation between dynamic patterns of peripheral CD4+ α4β7+ T-cell levels at week 24/28 and memory CD4+ α4β7+ levels, total HIV-DNA, assayed by FLIP-seq, and HIV-RNA levels at week 24. **(c)** Correlation between peripheral CD4+ α4β7+ T-cells and total, intact and defective HIV-1-DNA, assayed by FLIP-seq, at week 24. CD4+ α4β7+ levels were considered to decrease when there was >2.5 fold reduction at week 24/28 compared to BL. CD4+ α4β7+ levels were considered to increase when there was >1.3 fold change at week 24/28 compared to BL. **(d)** Dynamic of α4β7 expression on CD4 T-cells in ileum and caecum at BL and week 24. **(e)** Total cell-associated HIV-1-DNA and RNA in peripheral CD4+ T-cells α4β7+ and α4β7- sorted cells at BL and week 24. Horizontal red line indicates the limit of detection. P values were computed using Wilcoxon, Mann-Whitney U and Spearman test. Abbreviations: BL, baseline; W, week and ATI, analytic treatment interruption.
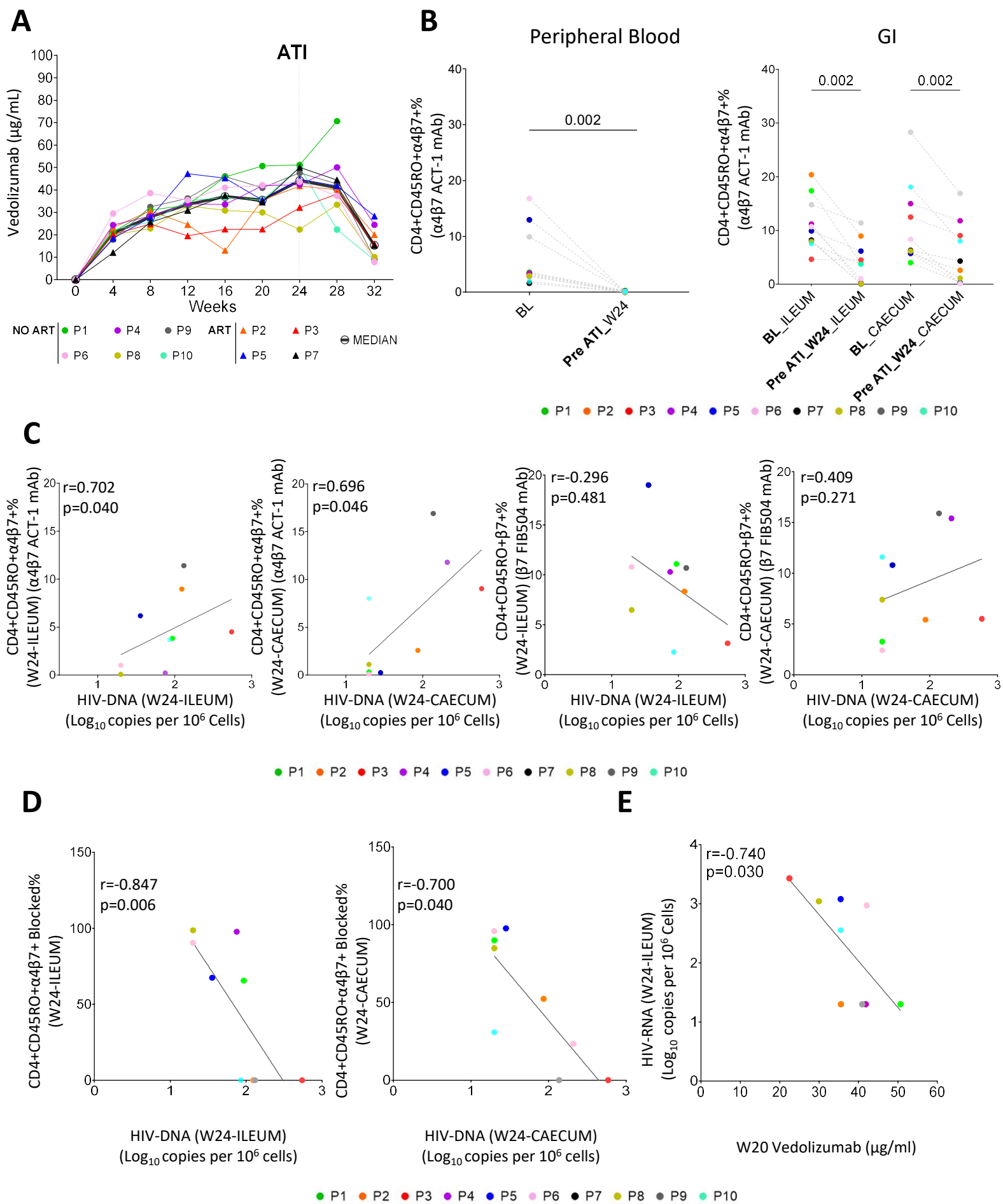
Fig. 5. Inefficient α4β7 blocking in GITs is associated with HIV-1 reservoir levels. (a) Serum concentration of vedolizumab along the follow-up. **(b)** Percentage of α4β7 integrin on peripheral CD4+ T-cells and on ileum and caecum CD4+ T-cells at BL and week 24. **(c)** Association between α4β7 expression on CD4 T-cells and HIV-1 reservoir at ileum and caecum before ATI (week 24). **(d)** Correlation between the percentage of α4β7 integrin blocked by vedolizumab and HIV-1-DNA reservoir at ileum and caecum. **(e)** Correlation between serum concentration of vedolizumab and HIV-1-RNA on ileum before ATI (week24). P values were computed using Wilcoxon, Mann-Whitney U and Spearman test. Abbreviations: BL, baseline; W, week and ATI, analytic treatment interruption.
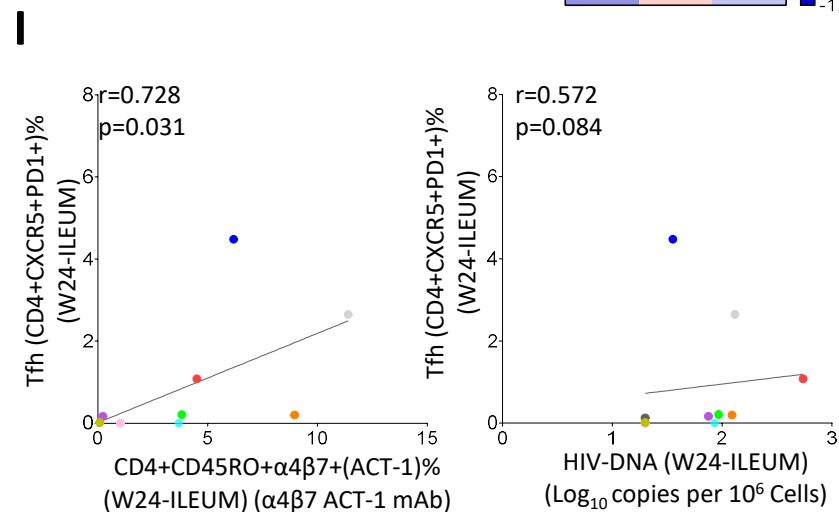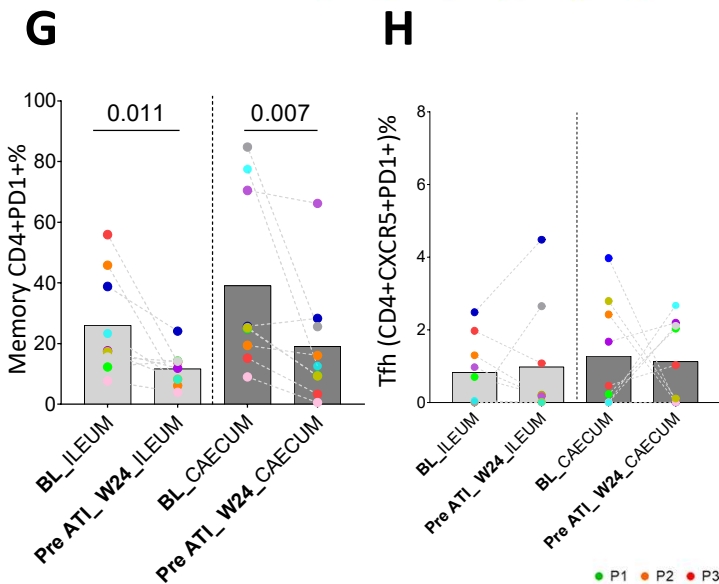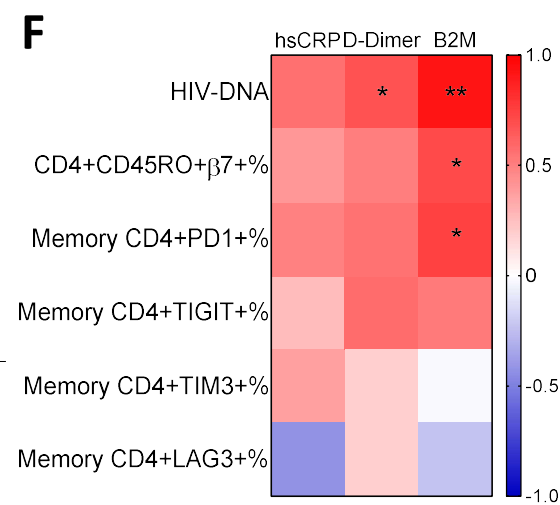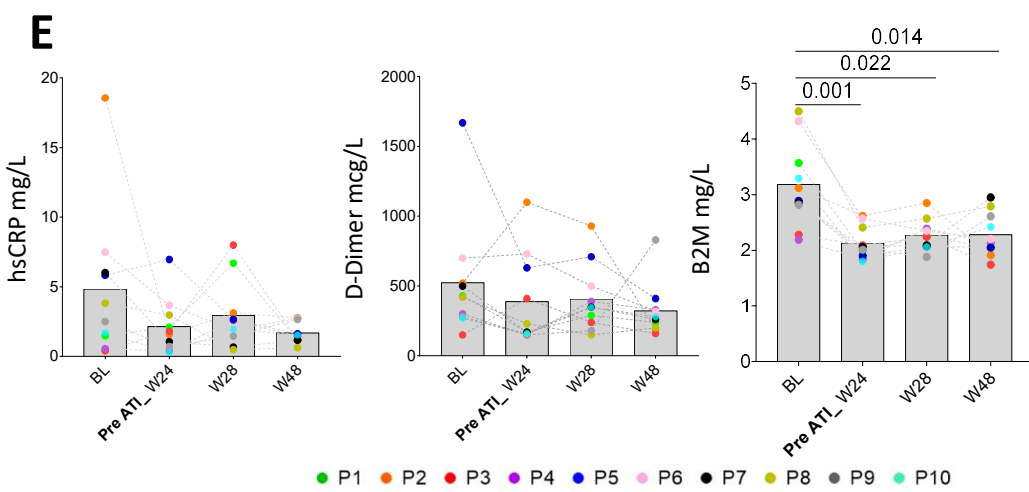
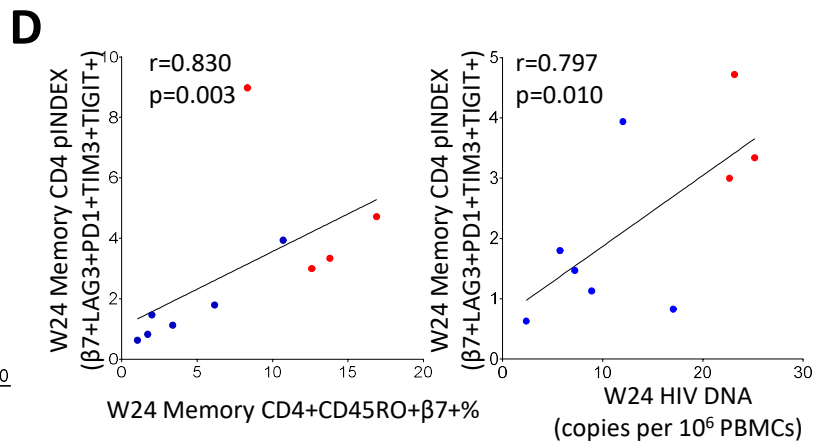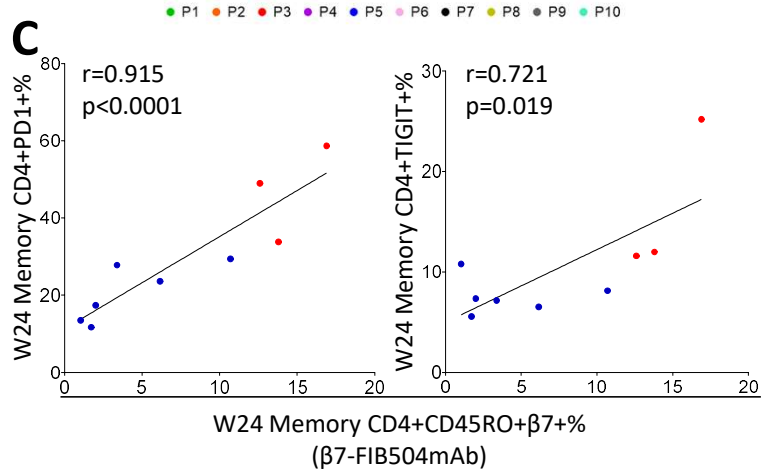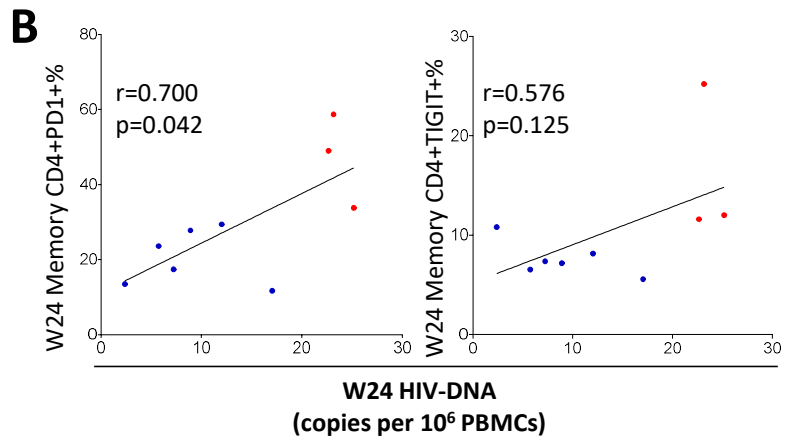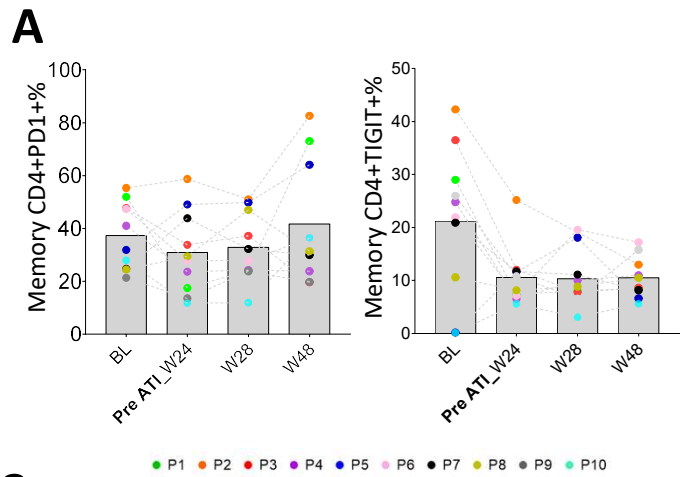**Fig. 6. Immune checkpoint molecules are associated with α4β7 and HIV-1 reservoir levels. (a)** Dynamic of PD1 and TIGIT expression on CD4 T-cells along the follow-up in PBMCs. **(b)** Correlation between total HIV-1-DNA levels, assayed by FLIP-seq, and the expression of PD1 and TIGIT on peripheral CD4+T-cells before ATI. **(c)** Correlation between the expression of α4β7 integrin and the immune checkpoint molecules (PD1 and TIGIT) on peripheral CD4+T-cells before ATI. **(d)** Correlation between the expression of α4β7 integrin and total HIV-DNA in PBMCs, assayed by FLIP-seq, and the simultaneous expression of α4β7, LAG3, PD1 and TIM3 on peripheral CD4+ T-cells just before ATI. **(e)** Plasma soluble biomarkers levels, hsCRP, D-Dimer and B2M, along the follow-up. **(f)** Correlation matrix representing negative (blue shading) and positive (red shading) association between soluble biomarkers and HIV-1-DNA in PBMCs, the expression of α4β7 and immune checkpoint molecules on CD4+ T-cells. **(g)** Dynamic of PD1 expression on CD4 T-cells at ileum and caecum at BL and before ATI (week 24). **(h)** Dynamic of CD4 Tfh at ileum and caecum at BL and before ATI (week 24). **(i)** Association between Tfh and CD4+ α4β7+ T-cells and HIV-1-DNA at ileum before ATI (week 24). P values were computed using Friedman test with Dunn's multiple comparisons test correction, Wilcoxon and Spearman test. Abbreviations: BL, baseline; W, week; ATI, analytic treatment interruption; Tfh, T follicular helper cells.
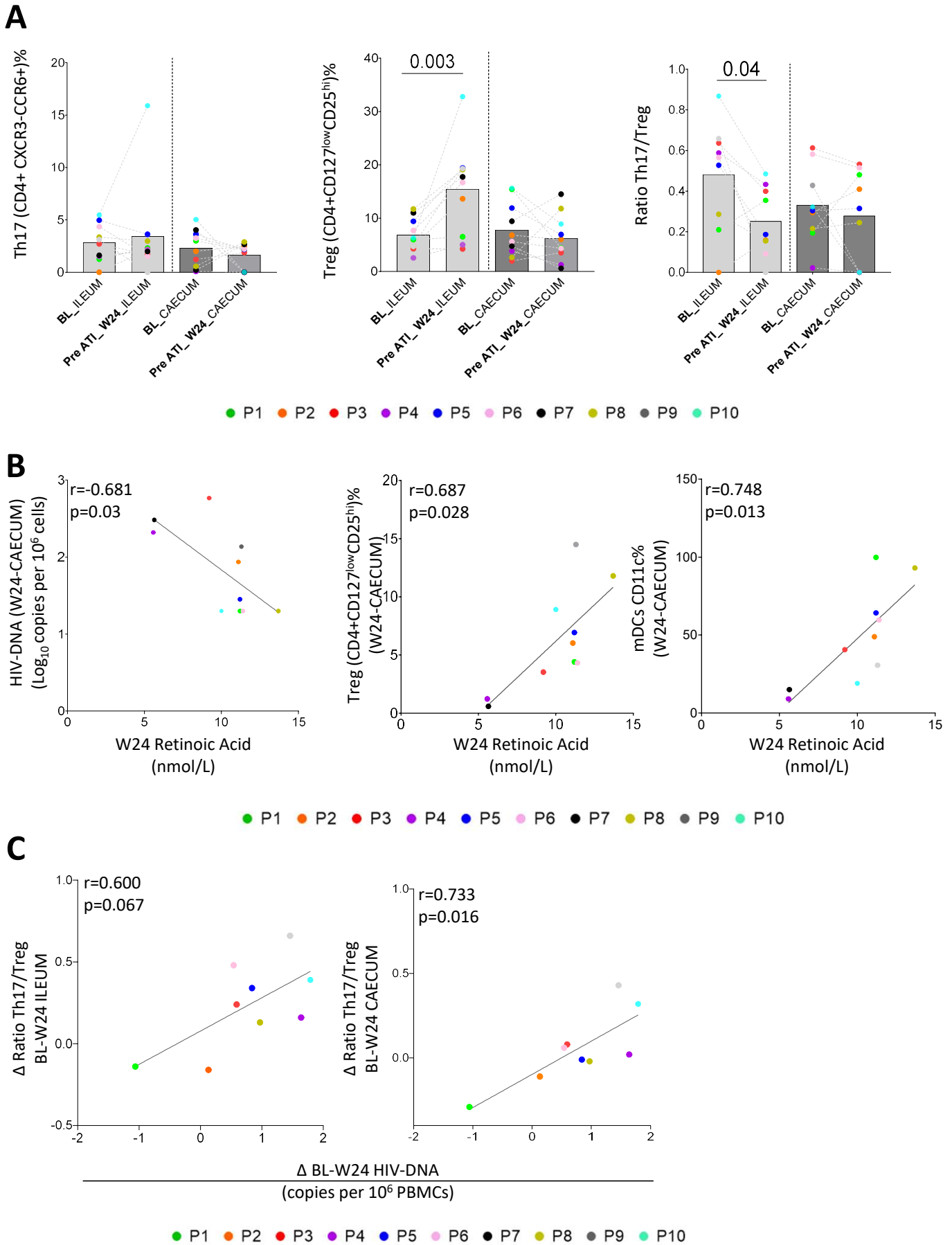
Fig.7. Retinoic acid plasma levels are associated with reservoir levels in GITs. (a) Dynamic of Th17, Tregs and Th17/Treg ratio at ileum and caecum along the follow-up. **(b)** Association between retinoic acid plasma levels and HIV-DNA, Tregs and mDCs at caecum before ATI (week 24). **(c)** Direct association between the dynamic of HIV-1-DNA reservoir in PBMCs and the Th17/Treg ratio at ileum and caecum before ATI (week 24). P values were computed using Wilcoxon and Spearman test. Abbreviations: BL, baseline; W, week; ATI, analytic treatment interruption; Treg, regulatory T cells; Th17, IL-17 producing T helper cells.